Genesis Minerals (Laverton) Limited

MMGO TSF Project Solute Transport Modelling

Numerical Groundwater Model.

penningtonscott
securing your water future

Genesis Minerals (Laverton) Limited

MMGO TSF Project Solute Transport Modelling

Numerical Groundwater Model.

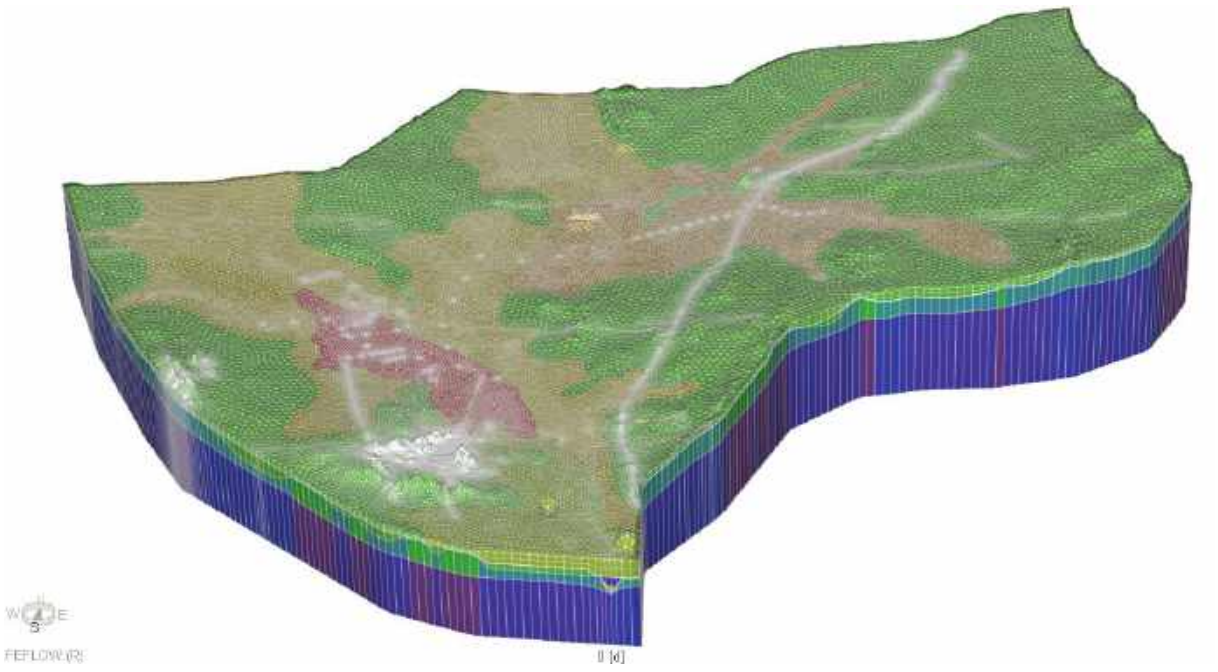

2469 | Rev 0
10 Nov 2025

Pennington Scott ABN 76 747 052 070
50 Edward Street
Osborne Park, WA 6017
T + 61 (0) 8 6272 0200

EXECUTIVE SUMMARY

During the previous operational phase of the Mt Morgans Gold Operation (**MMGO**) from March 2017 to March 2023, Dacian Gold deposited tailings from the 3 Mtpa Jupiter processing plant into Tailings Storage Facility (**TSF**) Cells 1 and 2. Genesis Minerals Limited (**Genesis**) recommissioned the Jupiter Plant in October 2024 and plans to increase throughput to 5 Mtpa by 2027. The TSF Project involves additional wall raises on Cells 1 and 2 and the construction of three new cells: Cell 3, Cell 2B, and the Mt Marven Cell. While Works Approvals have been issued for the Cell 1 and 2 raises, the new cells require further environmental and social impact assessment.

Seepage infiltration creates localised groundwater mounding beneath and immediately surrounding each TSF cell, with groundwater then migrating laterally toward zones of lower hydraulic head. Although TSF seepage (at 50,000 mg/L 120,000 mg/L) is less saline than that of the salt lake receiving environment (250,000 to 300,000 mg/L), it can contain additional solutes such as weak-acid dissociable (WAD) cyanide, nitrates, and trace metals. Metals tend to precipitate out of solution or adsorb to clays and organic matter within short distances of the TSF, whereas conservative (non-reactive) solutes, particularly chloride and nitrate, remain mobile and migrate the furthest along flow paths, with attenuation governed primarily by advection and dispersion processes.

To evaluate the fate and transport of the worst-case conservative solutes from the TSF, an existing regional groundwater flow model of MMGO dewatering and supply operations (Pennington Scott, 2025) was modified to simulate seepage and solute transport associated with the progressive development of all TSF cells. The model domain covers the MMGO restart period from October 2024 to October 2037 and assesses potential impacts on the surrounding hydrogeological system, including any risk to the Healing Pool.

The modelling was undertaken using the FEFLOW finite-element code to simulate coupled groundwater flow and solute transport, adopting an Equivalent Porous Medium (EPM) approach in which fracture networks are represented as zones of enhanced hydraulic conductivity within a porous matrix. Model geometry and hydraulic parameters were derived from the conceptual site model (CSM) described in Pennington Scott (2025), supported by borehole logs and the prior calibration dataset.

A base seepage rate of 530 m^3/day per cell was applied, consistent with CMW Geosciences (2024), with sensitivity simulations using multipliers of 1.5×, 2×, 3× and 4× to evaluate potential variability under different operational and hydraulic conditions. Solute transport was modelled conservatively (without retardation or chemical reactions) using a low effective porosity (n_e = 0.03), representing a worst-case scenario that maximises advective transport.

Sensitivity analyses show that higher seepage rates produce broader solute plumes extending predominantly southward and westward toward the dewatered pits, without altering the general direction of migration. Results are also sensitive to effective porosity: higher n_e values (~0.30) confine solute movement largely beneath the TSF footprint, whereas lower values (0.01–0.03) accelerate transport toward the pits. The adopted n_e = 0.03 aligns with measured specific-yield

values (2–3%) and provides a conservative representation of potential solute migration through the low-porosity fractured rock system.

Key findings from the solute transport modelling are summarised as follows:

- Migration direction: Solute transport from TSF Cells 1 and 2 occurs predominantly southward toward the Double Jay and Heffernan's Pits within the Jupiter Pit Complex, which functions as the principal hydraulic sink under continued dewatering.
- Hydraulic interception: Toe drains and collection sumps along the southern TSF embankments capture a portion of seepage; however, they do not fully offset the persistent drawdown gradients that drive groundwater flow toward the pits.
- Limited eastward migration: Solute movement toward the Healing Pool is negligible due to the very low transmissivity and subdued hydraulic gradients within the playa sediments and Lower Saprolite, combined with effective local drainage pathways.

In summary, even under highly conservative assumptions; including use of non-reactive solutes, elevated seepage rates, and low effective porosity, solute migration remains hydraulically constrained within the Jupiter Pit dewatering cone. The modelling indicates a very low likelihood of off-site migration under current or reasonably foreseeable operating conditions, and no credible pathway for solute movement toward the Healing Pool.

CONTENTS

LIST OF FIGURES

LIST OF TABLES

1. BACKGROUND

In 2023, Dacian submitted an application to the Department of Energy, Mines, Industry Regulation and Safety (DEMIRS) seeking approval to raise the crest elevation of Tailings Storage Facility (TSF) Cells 1 and 2 from RL414 m to RL418 m, and to construct a new embankment for a third cell (Cell 3), providing approximately 6.8 Mt of additional tailings storage capacity for the 3 Mtpa Mt Morgans Gold Operation (**MMGO**), located approximately 37 km WSW of Laverton, Western Australia (**Figure 1-1**).

The Department of Water and Environmental Regulation (**DWER**) subsequently issued Works Approval W2910/2025/1 under Part V, Division 3 of the Environmental Protection Act 1986 (WA) to facilitate the TSF expansion, including associated monitoring requirements.

In October 2024, ownership of MMGO transferred from Dacian to Genesis Minerals (Laverton) Pty Ltd, a wholly owned subsidiary of Genesis Minerals Limited (**Genesis**). Genesis now proposes to increase processing throughput from 3.0 Mtpa to 5.0 Mtpa. The expansion includes construction of additional TSF infrastructure, specifically Cells 2B and Mt Marven Cell.

For the purposes of this report, the progressive development of all TSF cells (Cells 1, 2, 3, 2A and Mt Marven), including both the previous operational period (2018–2023) and the projected thirteen-year future period to 2037, will hereinafter be referred to as the **TSF Project**.

Pennington Scott (2025) submitted a comprehensive H3 Hydrogeological Investigation Report to DWER in support of licence approvals for expanding MMGO's water supplies. This assessment included development of a regional groundwater simulation model, calibrated against historic mine dewatering, borefield abstraction, and TSF recharge observations during the Previous Operational Period (2017 to 2023), and forward-looking water supply predictive feasibility and impact simulations to 2035.

Genesis has now engaged Pennington Scott to refine the existing MMGO groundwater model to incorporate solute transport and particle-tracking simulations for the progressive development of the proposed TSF cells to 2037. This work will ensure the TSF Project does not result in unacceptable, serious, or irreversible impacts on environmental or social values.

The contained document represents TSF solute transport Numerical Groundwater model for the Mount Morgans Gold Operation prepared to assist in obtaining works approval.

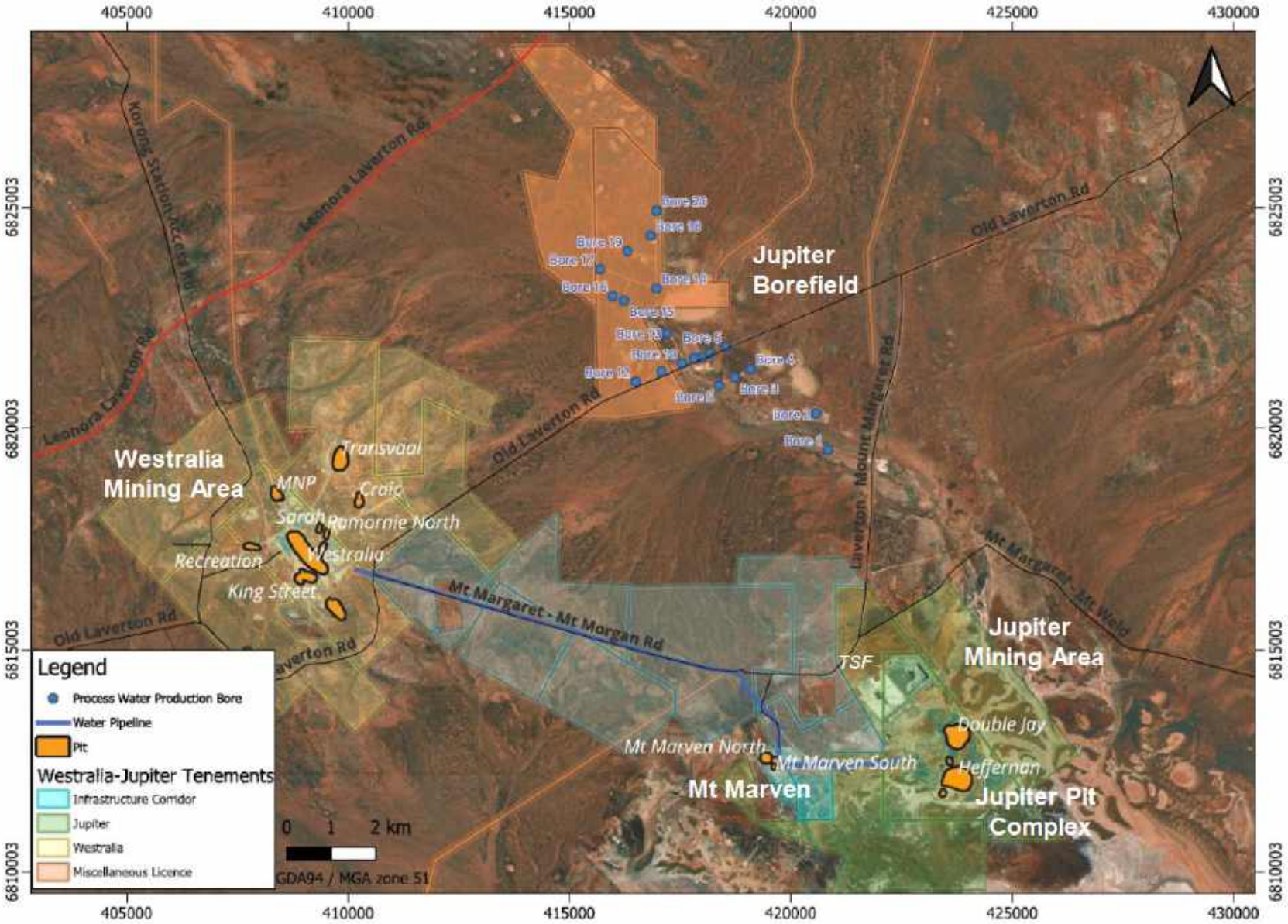

Figure 1-1 MMGO location plan.

1.1 Conceptual Site Model of the TSF

The regional conceptual site model (CSM) for MMGO used in the current study is discussed in detail in Pennington Scott (2025b), however this section addresses hydrogeological conditions specifically around the TSFs.

Historical investigations around the TSF

The existing TSF Cells 1 and 2 were developed by Dacian Gold during the previous operational phase of MMGO between March 2017 and March 2023. Following an operational hiatus of approximately 18 months, the TSF was recommissioned by Genesis Minerals in October 2024.

Pennington Scott (2024) reported that the original drilling logs for Dacian's monitoring bores TSFMB01 to TSFMB06 have been lost. However, in 2024 Genesis constructed seven seepage recovery bores (TSFAB04–TSFAB10) and one additional monitoring bore (TSFMB07) around the two TSF cells, as shown in **Figure 1-2.**

Drilling logs from these new bores indicate that TSF Cells 1 and 2 are underlain by a very thin veneer of colluvial and/or lacustrine (salt lake) sediments. In most bores, this veneer is only 1–2 m thick; however, in bores TSFAB09 and TSFMB07, the thickness increases to 6 m and 11 m, respectively. Notably, in these latter bores the upper 3 m comprises coarse, permeable sand overlying less permeable interbedded lacustrine clayey sand and silt/clay horizons (Pennington Scott 2025a).

Beneath these thin transported and residual sediments lies Archean (4,000–2,500 Mya) mafic igneous bedrock, which exhibits negligible primary porosity or permeability characteristics. Groundwater within this bedrock occurs and flows through secondary porosity developed within open joint networks in the 20–30 m thick Lower Saprolite weathering horizon (commonly referred to as the *zone of joint oxidation*). A smaller proportion of groundwater flow is transmitted via preferential pathways developed in major faults, shear zones, and fracturing within the otherwise impermeable fresh crystalline basement. The proportion of the fresh rock that contains fractures or joints capable of transmitting groundwater is referred to as the Saprock, or the transition zone. The Saprock zone typically extends to about 90 mBGL, albeit there are cases in the literature where the Saprock extends to depths of up to 200 m.

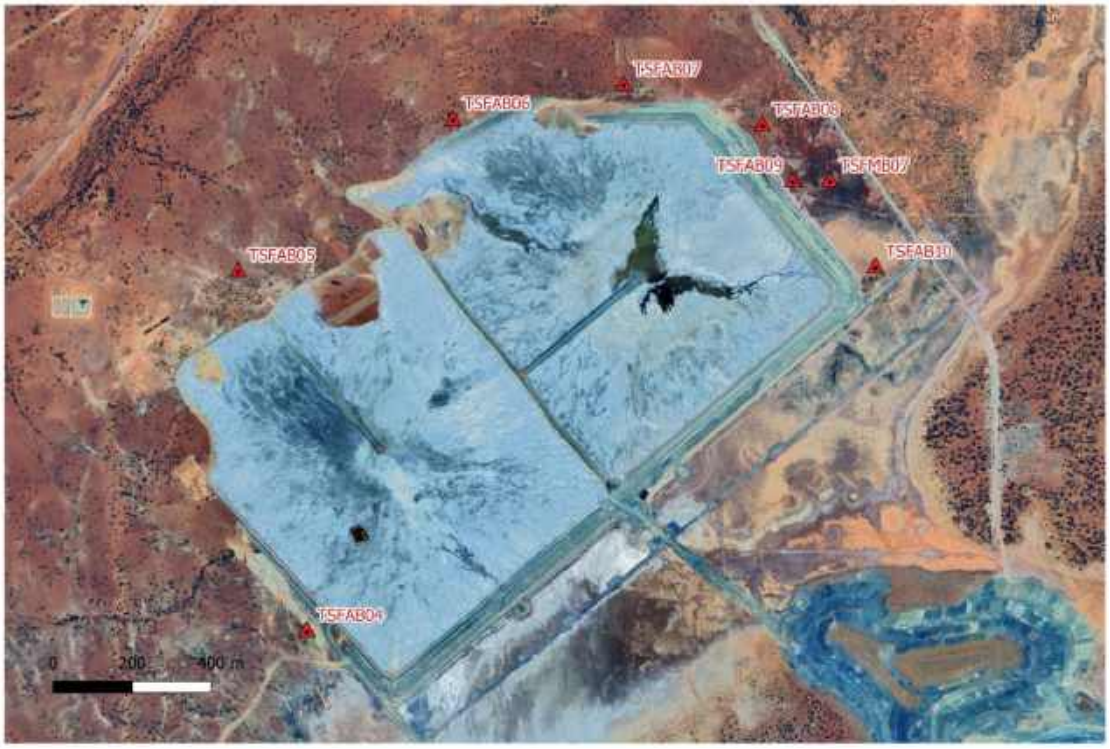

Figure 1-2 **Locality of the TSF bores (marked in red) at the Mount Morgans TSF Project**

Groundwater migration pathways from the TSFs

From a hydrogeological perspective, the open water area in the decant pond atop the TSF cells represents a fixed water head whenever tailings are being actively deposited to the cell. The tailings and the underlying veneer of clayey transported sediments have low permeability and represent vertical hydraulic impedance limiting the rate of vertical seepage losses from the TSF Cell. The vertical impedance in this study is calibrated based on the seepage rates from CMW (2024).

Once seepage enters the aquifer, groundwater migrates laterally, preferentially through the Lower Saprolite. A smaller proportion of flow may be diverted along major structural features, including a north–south shear zone and the fractured margins of an east–west–trending dolerite dyke that intersects Cells 1 and 2.

Both the salt lake along the southern boundary of the TSF cells and the Jupiter Pit Complex function as regional groundwater sinks. As groundwater flows laterally through the Lower Saprolite toward these discharge zones, a proportion of this flow is forced upward under artesian pressure through the low permeability lacustrine (playa) deposits toward the lake surface. Evaporative discharge then occurs once the water table rises within approximately 2 m of ground level, where capillary rise can transport groundwater into the **capillary fringe**, allowing direct evaporation from shallow pore spaces.

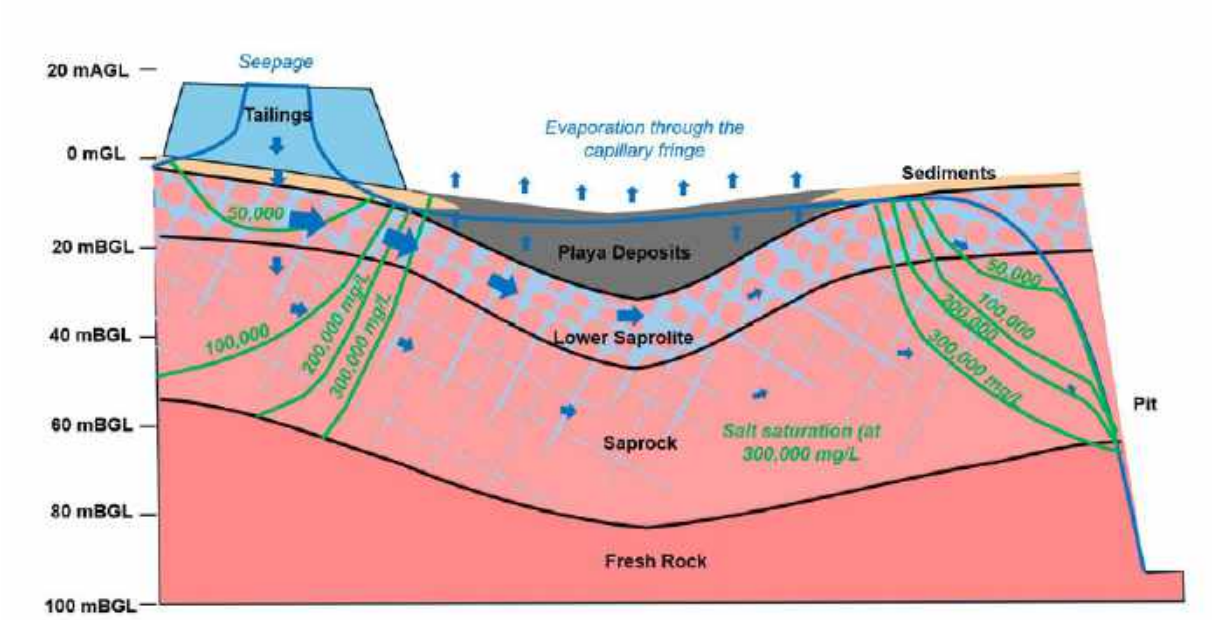

Figure 1-3 Schematic CSM of solute migration from the TSF to the Jupiter Pit Complex

Solute fate and transport mechanisms

The process water discharged to the TSF is not hypersaline; it is sourced primarily from the brackish Jupiter Borefield within the Calcrete Aquifer, with salinity typically below 14,000 mg/L. In contrast, salt efflorescence observed around the salt lake on the southern boundary of the TSF (Figure 1-2) indicates that local groundwater salinity there is at or above the salt-solubility limit (270,000–320,000 mg/L), beyond which salts naturally precipitate from solution. Even with the future incorporation of hypersaline palaeochannel water sources, Genesis will blend (shandy) process water to maintain an operational salinity below approximately 120,000 mg/L to minimise reagent consumption and operating costs. Accordingly, TSF seepage will consistently remain less saline than the salt-lake receiving environment (Pennington Scott, 2025b).

Salinity alone is not the concern with TSF seepage, however. TSF water may contain additional solutes such as weak-acid dissociable (WAD) cyanide, nitrate, and trace metals, and understanding their fate and transport once they enter the groundwater system is essential.

Once seepage infiltrates beneath the TSF, each parcel of solute displaces the groundwater previously occupying that pore space, which in turn displaces the next parcel along the flow path. This displacement mechanism (piston flow) creates a sequential push-through migration

of groundwater and solutes. Under piston-flow conditions, a hydraulic pressure response in the confined lower saprolite aquifer may propagate rapidly over considerable distances; however, the actual solute mass responsible for the pressure change has moved only a short distance from its point of entry. In effect, the pressure signal travels far faster than the contaminant mass itself.

Different solutes also exhibit fundamentally different behaviours once in the subsurface. Advection, dispersion, adsorption, and precipitation are the key processes controlling solute transport and transformation. Advection transports solutes with the bulk movement of groundwater, while dispersion spreads solutes through molecular diffusion and mechanical mixing along heterogeneous flow paths. Adsorption involves the attachment of solutes onto mineral surfaces, and precipitation occurs when dissolved constituents exceed their solubility limits and transition into solid mineral phases.

For example, WAD cyanide is readily oxidised to nitrate upon exposure to acidic conditions or ultraviolet light. Trace metals (particularly if present in WAD cyanide complexes) are reactive and typically precipitate as oxide-hydroxide phases or adsorb strongly to clay minerals and organic matter within short distances of the TSF, restricting their mobility. By contrast, conservative (non-reactive) solutes such as chloride and nitrate remain mobile and migrate further along flow paths, with attenuation governed almost entirely by advection and dispersion.

To quantify the fate and transport of the most conservative solutes under worst-case conditions, this study modifies the existing regional groundwater flow model of MMGO dewatering and supply operations (Pennington Scott, 2025). The enhanced model simulates seepage and solute transport associated with the progressive development of all TSF cells over the MMGO restart period from October 2024 to October 2037, assessing potential impacts on the surrounding hydrogeological system, including any risk to the Healing Pool.

2. MODEL DESIGN

Numerical groundwater models are a powerful tool for evaluating spatial and temporal variability in aquifer response (e.g., water levels, abstraction effects, mine dewatering, and flux distribution). When properly constructed, they support rigorous sensitivity and uncertainty analysis and enable evaluation of natural and operational stresses within a transparent, defensible framework.

This numerical groundwater model provides a quantitative implementation of the current hydrogeological understanding for the site, as defined in the Conceptual Site Model (**CSM**) (Pennington Scott, 2025). The first model iteration (Version 1) was developed to characterise aquifer behaviour across the project area and evaluate groundwater supply options that ensure long-term borefield sustainability while protecting stygofauna habitat within the Priority Ecological Conservation Area.

The viability of the stygofauna ecosystem depends on maintaining groundwater levels above ecological thresholds within the Calcrete aquifer. The model was also used to assess potential impacts on groundwater conditions at the Healing Pools, a culturally and environmentally sensitive receptor area. While such assessments can be undertaken using analytical techniques, analytical approaches are typically limited in complex hydrogeological settings and may introduce significant uncertainty. In contrast, numerical modelling provides a more robust representation of subsurface conditions and groundwater processes, consistent with available site data.

Version 2.1 (this report) builds directly on the calibrated Version 1 model, adopting the same aquifer properties, boundary conditions, and pumping stresses. The key objectives of the contained groundwater modelling for the TSF program are to:

- **Simulate current and future groundwater conditions around the TSF** under existing and proposed abstraction scenarios within the Calcrete and palaeochannel aquifers. (Completed in Version 1; Stage 3 pumping stresses from Scenario 4 in Pennington Scott, 2025 are also carried forward here.)
- **Assess solute transport from the TSF Project**, including plume migration pathways, seepage rates, and potential interactions with environmental and mine-related receptors.
- **Evaluate sensitivity and uncertainty around the TSF Project**, identifying key hydrogeological parameters affecting flow and transport behaviour and informing monitoring, adaptive management, and regulatory validation.

Version 2.1 of the MMGO model (this report) builds directly on the calibrated Version 1 model, adopting the same aquifer properties, boundary conditions, and pumping stresses. Key updates include:

- expansion of the model domain to incorporate the proposed Stage 3 borefield in the up-gradient Laverton Gold Project (**LGP**) sector

- refinement of the model grid around the TSF to simulate seepage and solute-transport mechanisms
- implementation of contaminant-transport modelling to assess plume migration pathways and potential receptors

Unlike the previous numerical modelling, this modelling phase focuses on solute-transport scenarios. Pumping assessments for the Stage 3 borefield will be undertaken in a future model update once drilling and pump-testing results become available.

This study uses FEFLOW, an industry-standard finite-element groundwater modelling platform selected for its capability to simulate variably saturated flow and advective-dispersive solute transport by solving the continuity equation and Darcy's Law.

2.1 Model selection

Groundwater modelling science (Anderson, Woessner, & Hunt, 2015) and relevant guidelines (Barnett, et al., 2012) suggest justification of the numerical-code selection based principally on the modelling objectives, the aquifer characteristics, and the functionality and performance features of the computer code (Heijde, 1996).

Examples of performance and functionality criteria include among others, the computer interface (**GUI**), the ability of the code to simulate steep gradients at hydraulic or natural geological boundaries (e.g. pumping well), desaturation and re-saturation of model cells or elements, simulation capacity of various parameters and state variables (such as ground water levels, fluxes, pressure and quality), flexibility in time-changing aquifer properties and boundary conditions flexibility on data assimilation and processing by means of programming interface, postprocessing of modelling results, etc.

Based on the review and analysis of site-specific conditions, available data and modelling objectives, the numerical code selected for the development of this model was the latest version of the industry-standard Finite - Element DHI-WASY code **FEFLOW**.

2.2 Model domain and mesh design

The hydrogeology of the model area suggests a layered aquifer arrangement, with most of aquifer storage in the Calcrete aquifer, and the Werillup formation in the Palaeochannel. The weathered bedrock and the Lower Saprolite offer minor storage diminishing with depth. The fresh-rock exhibits very low permeability and virtually no significant storage and yield. The bedrock formations are intersected by a number of vertical structures, mainly dykes, the shear zone, and other fracture-fault zones. The aquifer hydrostratigraphy consists of the Upper deposits, a layer succession that comprises the palaeochannel deposits, and the underlying bedrock sequence, which consists of the Upper Saprolite, the Lower Saprolite, the Saprock, and the fresh bedrock

The finite element method implemented by FEFLOW requires discretisation of the modelled area into a mesh of triangular elements defined by a series of node locations. Solutions are obtained for potentiometric head at each nodal point within the model domain and is

interpolated within the entire area of each model element by interpolation functions based on Galerkin method.

For the needs of this project, the model domain was expanded to the northeast to include the stage-3 borefield and was also further refined in the TSF area to more accurately simulate the seepage and the contaminant transport. The updated model domain covers the above aquifer system over an area of 1547 square kilometres, which has been discretised into a finite element mesh consisting of 101,769 elements and 51,130 nodes per model layer/slice, totalling 712,383 elements and 409,040 nodes over the six model layers (**Figure 2-1**). The mesh is enhanced by way of increased nodal density within the pit areas, bore locations as well as at bores where pump testing was conducted. A multi-layered modelling approach has been adopted to accommodate stratigraphic complexity in the hydrogeological model. The size of the mesh elements ranges from as low as 20 m in the TSF area, about 40 m at bore locations, increasing gradually to about 400 m towards the periphery of the model domain. A refined element size of about 50 m was also at the structural features.

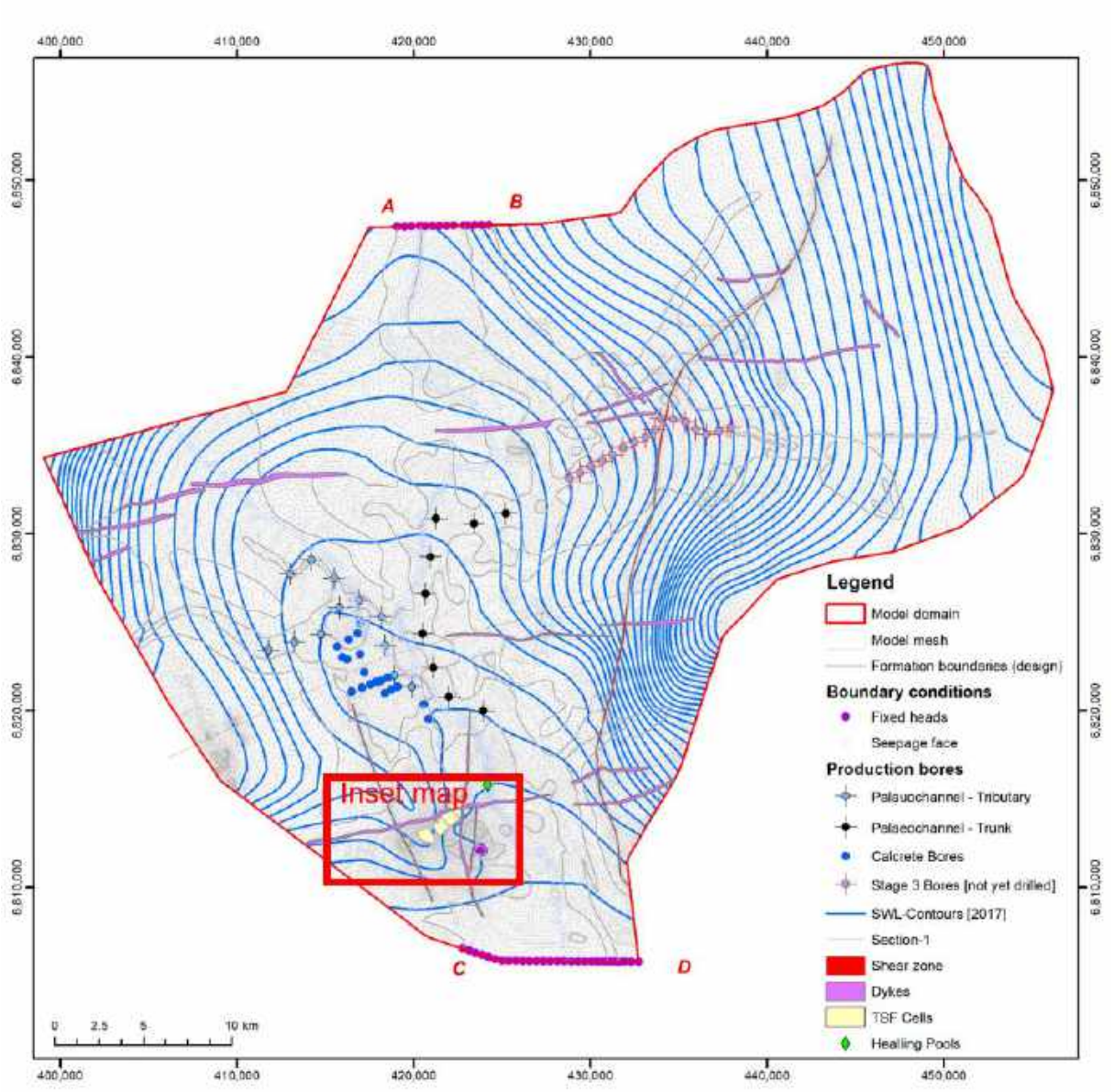

Figure 2-1 Finite element mesh and boundary conditions

The model mesh was created using a mesh generator based on the Advancing Front method (https://www.aquaveo.com/software) which, except for polygon topologies, honours the presence of linear and point features such as rivers, faults and pumping locations and pit boundaries. This methodology produces a finite-element mesh of smooth, equilateral and Delaunay triangles that contribute to model stability, minimizing numerical errors and reducing model runtimes. In terms of mesh quality, the final model mesh that was created in this project contains triangles that are mostly equilateral with zero violations of Delaunay criterion.

The model is discretised vertically into six model (hydrostratigraphic) layers as follows(**Figure 2-2,Figure 2-4**):

- **Layer 1**: Represents the upper sediments, which include the Calcrete, Alluvial, Fluvial, and Playa deposits.
- **Layer 2**: Represents the Perkolilli Formation.
- **Layer 3**: Comprises the Werillup Formation within the palaeochannel, transitioning into the lower Saprock beyond the channel boundaries.
- **Layer 4**: Comprises the lower Saprock.
- **Layer 5**: Represents the fractured bedrock (or upper Saprock), with an approximate thickness of 70 to 90 m, thinning along the axis of the palaeochannel.
- **Layer 6**: Represents the fresh bedrock, extending from the base of the Saprock to the model base at 100 m AHD

Layes 1 to 4 thin out to the outskirts of the plain, transitioning into various levels of the Saprock. **Figure 2-3** shows the details of the geometry of model layers.

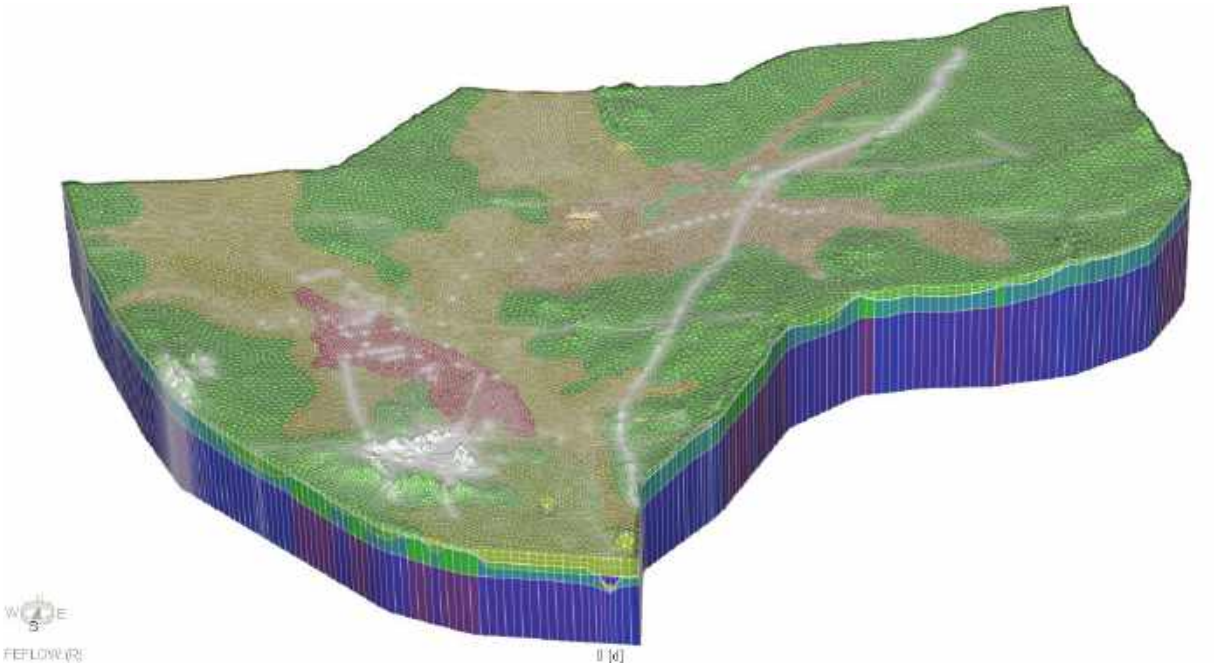

Figure 2-2 3D representation of the model mesh

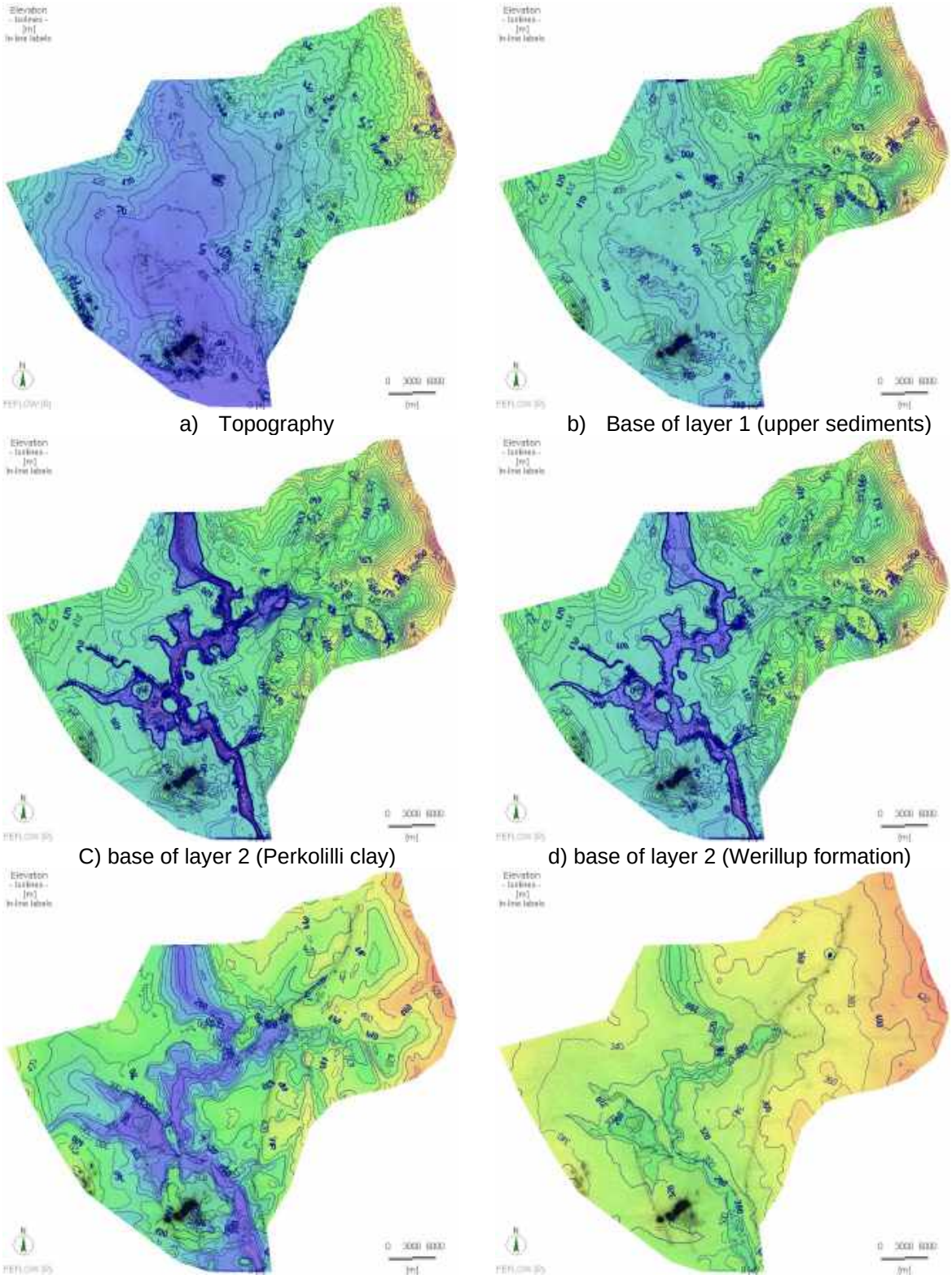

a) Topography

b) Base of layer 1 (upper sediments)

C) base of layer 2 (Perkolilli clay)

d) base of layer 2 (Werillup formation)

e) base of layer 4 (Lower Saprolite)

f) base of layer 5 (Saprock)

Figure 2-3 Geometry of the model layers

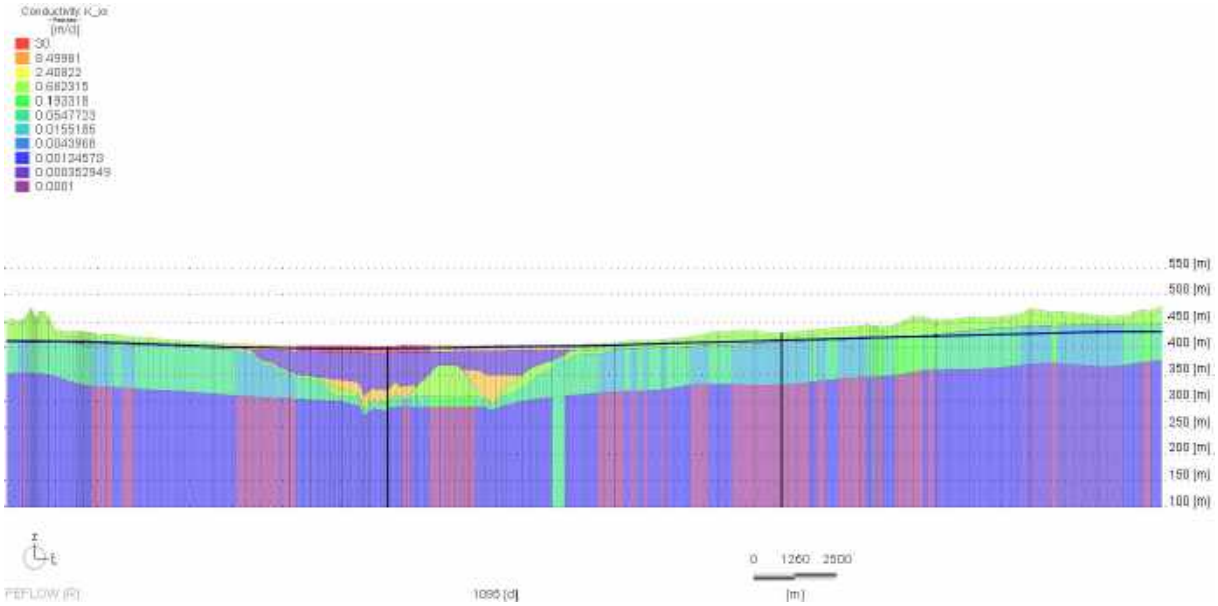

Figure 2-4 Model profile along section 1 (Figure 2-1)

2.3 Boundary conditions

The boundary conditions in the numerical model were assigned based on the major inflows and outflows identified in the CSM. As shown in **Figure 2-1**, a fixed-head boundary was applied along the northern (AB) and southern (CD) boundaries to represent lateral inflow from the upgradient areas and outflow to the downgradient areas, respectively. A no-flow boundary condition was applied elsewhere.

A seepage face boundary condition (i.e., first-type constrained or Dirichlet condition) was used along the major drainage network on the top model layer to represent seepage and evaporation losses.

3. MODEL CALIBRATION

3.1 Calibration methodology

This model is an extension of the previously calibrated Version 1 groundwater model (Pennington Scott, 2025), and has been developed primarily to simulate contaminant transport from the TSF cells to the surrounding aquifer system.

The current model retains the aquifer parameters (**Table 3-1**), boundary conditions, and pumping stresses adopted in Version 1, and builds directly on its successful steady-state and transient calibration, which reproduced observed hydrographs and regional groundwater flow patterns. Consequently, no additional calibration has been undertaken for this version.

This report focuses exclusively on solute-transport outcomes. Pumping scenarios for the Stage 3 future LGP Borefield(s) will be assessed in a future model update once drilling and pump-testing data become available. At that stage, further calibration and parameter refinement will be undertaken to integrate the new hydrogeological information.

3.2 Adopted aquifer - hydraulic properties

A summary of hydraulic parameters of different hydrostratigraphic units in the CSM are provided in **Table 2-1**, while **Figure 3-2** shows the parameter zones within each unit. Reference to this table suggests a high variability and relative uncertainty in the range of anticipated values of horizontal (**Kh**) and vertical (**Kv**) hydraulic conductivities for individual hydrostratigraphic units. A higher uncertainty is also associated with regards to the expected range of aquifer storativity (**S, Sy**). Conservative values of aquifer storage properties are selected at transient and predictive simulations based on experience from similar projects in the area.

Net groundwater recharge across the parameter zones was set up as a recharge-to-precipitation ratio (recharge ratio). The adopted recharge ratios for the different parameter zones are shown in **Figure 3-1.** Average recharge ratios are generally negligible, reflecting a worst-case scenario with regards to the drawdown impacts, and the model objectives. However, based on the conceptual model, higher recharge ratio can be anticipated over a recurrent period of about 10 years, mainly over the lake depressions.

Table 3-1 Adopted base hydraulic properties with the parameter zones in Figure 3-2

Layer	Zone	Kh	Kz	Ss	Sy
1	Calcrete	70	7	1.00E+05	0.08
	Alluvial	5	0.5	1.00E+05	0.05
	Fluvial	10	1	1.00E+05	0.05
	Playa	2	0.2	1.00E+05	0.02
	Saprolite	0.54	0.054	5.00E-06	0.01
2	Saprolite	0.54	0.054	5.00E-06	0.01
	Perkolilli Clay	0.0005	0.00005	1.00E-05	0.005
3	Werrillup	5	0.5	1.00E-05	0.03
	Saprolite	0.54	0.054	5.00E-06	0.01
	Saprock	0.05	0.005	5.00E-06	0.01
4	Saprock	0.02	0.005	5.00E-06	0.01
5	Granite	0.01	0.001	5.00E-06	0.01
	Mafic - Ultramafic	0.05	0.005	5.00E-06	0.01
	Felsic Vol	0.01	0.001	5.00E-06	0.01
6	Granite	0.0001	0.00001	1.00E-06	0.001
	Mafic - Ultramafic	0.001	0.0001	1.00E-06	0.001
	Felsic Vol	0.0005	0.00005	1.00E-06	0.001

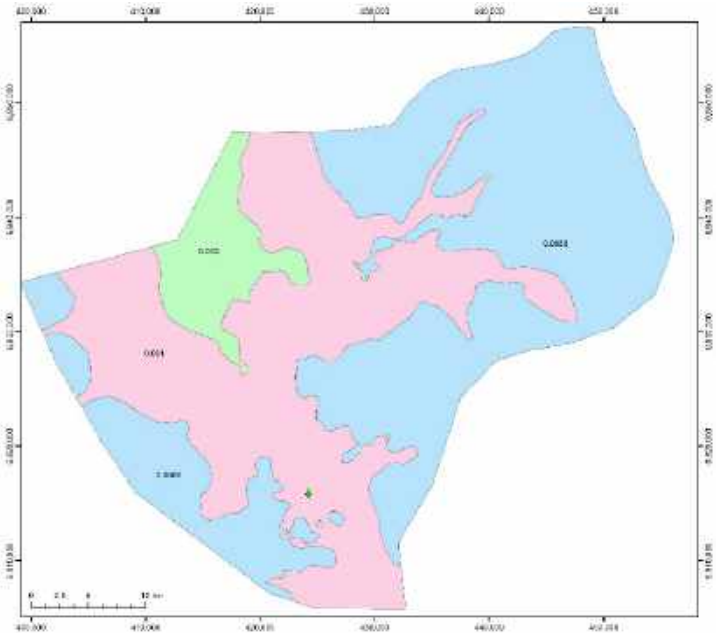

Figure 3-1 Adopted recharge to precipitation factors from Steady – state calibration

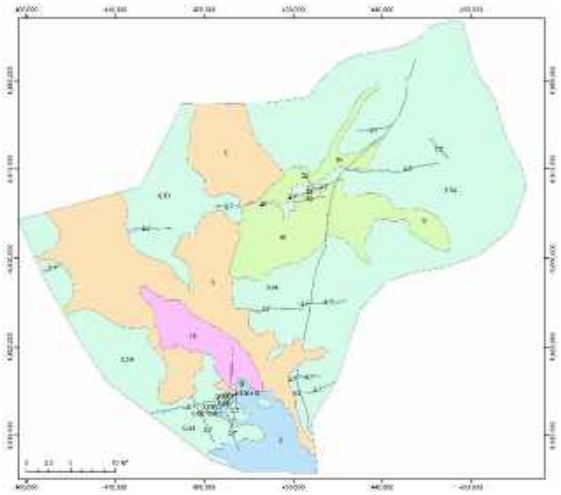

***Layer 1*: Upper Sediments, Saprolite**

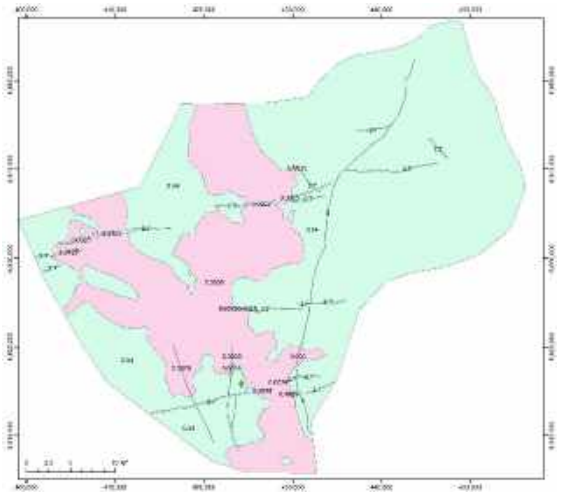

***Layer 2*: Perkolilli clay, Saprolite**

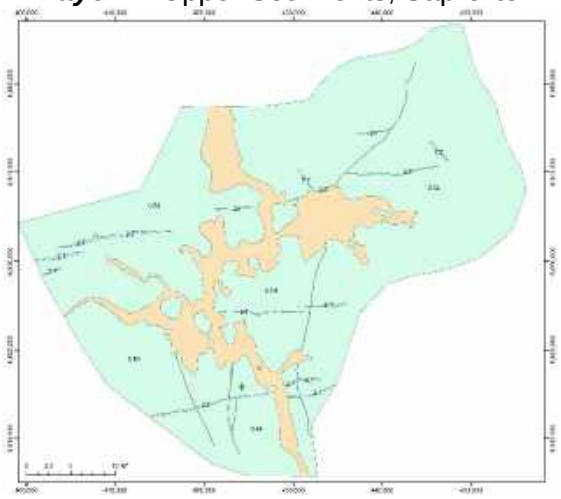

***Layer 3*: Werillup, Saprolite**

***Layer 4:* Lower Saprolite**

***Layer 5:* Saprock**

***Layer 6*: Fresh bedrock**

Figure 3-2 Horizontal hydraulic conductivity (Kh) zones at model layers

4. PREDICTIVE SCENARIOS – MODEL RESULTS

4.1 Model setup and assumptions

The purpose of this modelling assessment is to simulate solute transport associated with seepage from the TSF cells during the operational period from October 2024 to 2037. This requires establishing appropriate initial and boundary conditions for both groundwater flow and solute-transport processes to predict solute migration from the TSF to the surrounding aquifer system.

Solute transport may be represented using either (i) advective-only particle tracking or (ii) a full solute-transport solution. In this study, the latter approach is adopted, whereby solute concentration is treated as a state variable and the governing transport equation is solved explicitly, incorporating advection, hydrodynamic dispersion, and diffusion.

The model was implemented in two sequential phases:

- **Phase 1** - simulates the historic hydraulic conditions from 2018 to June 2025, for estimating the groundwater levels and contaminant concentrations for the predictive phase 2.
- **Phase 2** – is setup and run for the predictive period from July 2025 to the end of mining in October /2037.

Groundwater levels and solute concentrations calculated at the end of Phase 1 are used as initial conditions for Phase 2.

Phase 1 simulations commenced using hydraulic conditions representative of early 2018 (**Figure 4-1, Figure 4-2**). Groundwater levels at this time reflect the cumulative effects of repeated historical dewatering cycles, resulting in a persistent drawdown cone centred on the Jupiter Pit Complex (Double Jay and Heffernan's Pits).

Measured water levels in February 2020 indicated:

- Double Jay Pit: 320 m AHD
- Hefferan's Pit: 390 m AHD

In the model, the minimum groundwater level at the Joanne Pit was assumed equal to the base of the saprock (~315 m AHD), which was applied as a fixed-head boundary. Below this elevation, the formation transitions to fresh bedrock with extremely low hydraulic conductivity (**Table 3-1**), consistent with negligible recorded inflows to underground workings; thus, the bedrock was treated as effectively impermeable.

A steady-state calibrated model was first executed with the Double Jay fixed at 315 m AHD to define the initial hydraulic surface. The Heffernan's Pit was not fixed-head constrained, as its groundwater level (~390 m AHD) was correctly reproduced by model solution in response to hydraulic gradients imposed by the boundary condition at Double Jay.

The exact operational dewatering regime within underground mine workings was not explicitly simulated, as this falls outside the scope of the current model. The resulting groundwater elevation surface and pit-cell configuration used as initial conditions for Phase 1 are presented in **Figure 4-2**.

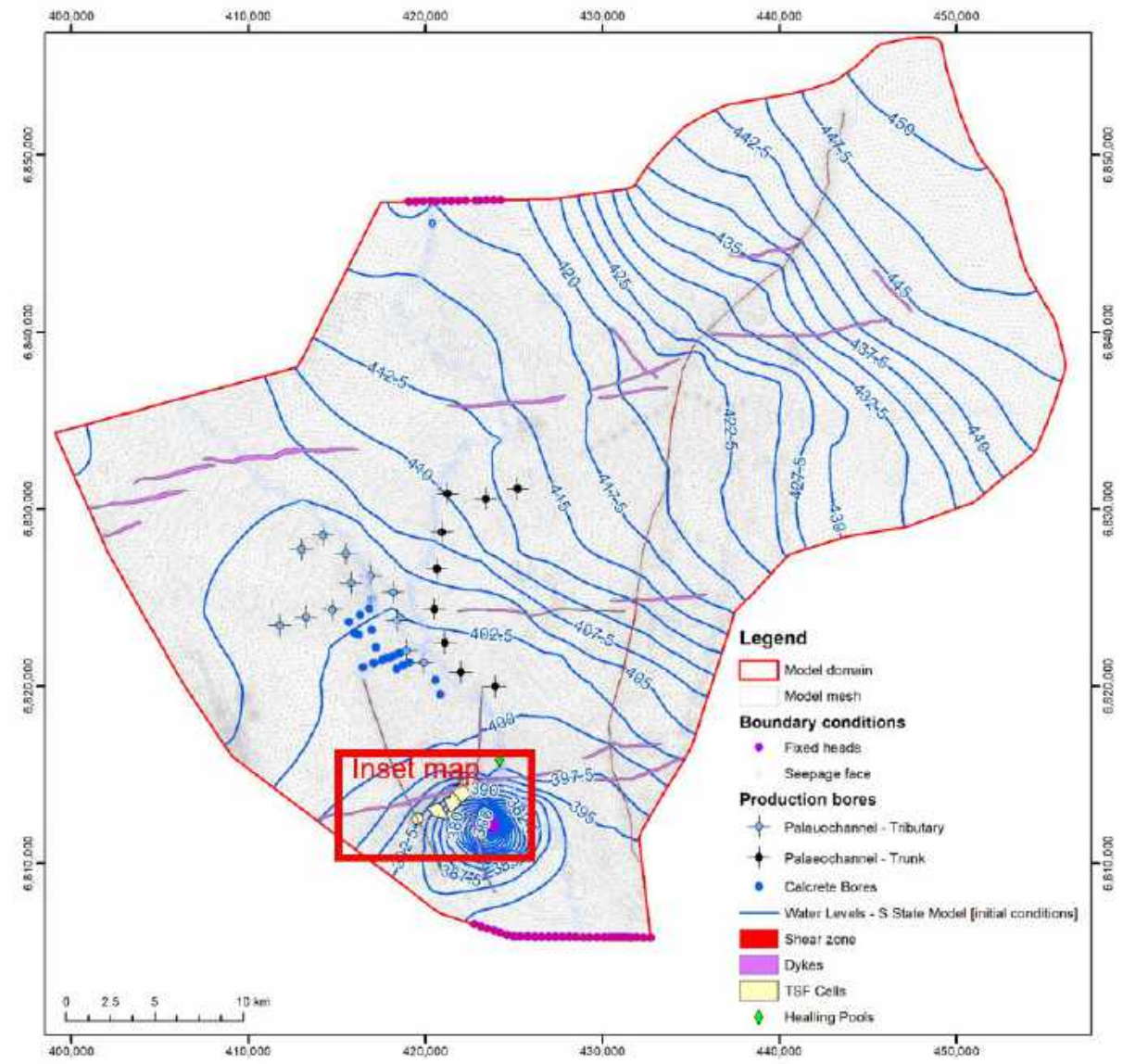

Figure 4-1 Initial groundwater levels used for transient state simulations.

According to the TSF geotechnical design report (CMW Geosciences, 2024), seepage from each cell during active operation is estimated at 529.4 m³/day, occurring over an average “pool area and running beaches” of 62,832 m². For modelling purposes, seepage is assumed to originate predominantly from the central pool area of each TSF cell, as shown in **Figure 4-2**..

Finite-element zones representing these pool areas were defined in the model, ranging from 58,607 m² in Cell 2 to 90,268 m² in Cell 4, while applying a consistent seepage rate of approximately 530 m³/day per cell (

Table 4-2). Distributing the same seepage volume across slightly larger footprints provides a conservative representation by allowing the contaminant source to be distributed over a broader area.

Although the actual position and geometry of the pool will vary over time in response to tailings deposition practices, the pool footprint in each TSF cell is assumed to remain fixed and centrally located for the purposes of this simulation.

With respect to the hydraulic properties of the underlying formations, the TSF design report adopted permeability values of 0.46 m/day for extremely weathered basalt, 0.05 to 0.5 m/day for playa deposits, and 0.01 m/day for saprolite clays. In the present model, higher hydraulic conductivities have been applied, specifically 0.54 m/day for saprock and 2.0 m/day for the playa deposits (refer to Table 2-1). These elevated values are considered conservative (worst-case), as they promote higher groundwater fluxes and therefore greater potential plume migration distances relative to design assumptions.

Tailings deposition was simulated following the operational schedule outlined in **Table 4-1** and **Figure 4-3**. Cell 2 (the easternmost cell) was activated first and, in the model, is assumed to remain continuously active throughout Phase 1, representing the period 2018 to mid 2025.

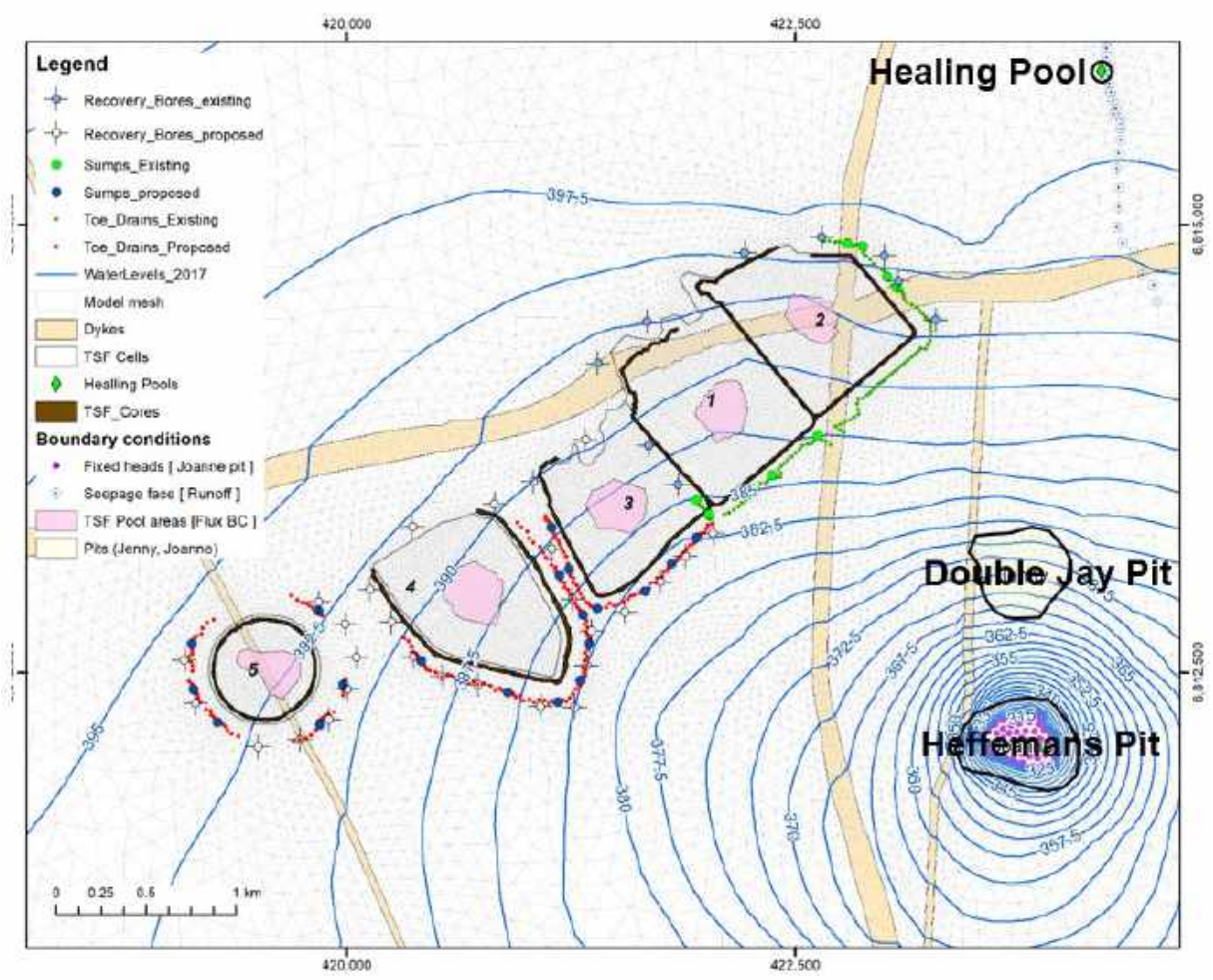

Figure 4-2 Setup of the TSF Cells, boundary and initial conditions of the model at the start of simulation in Jan 2018.

Table 4-1 Detailed listing of the deposition pattern in each TSF cell

Cell ID	Deposition	RL Base (m AHD)	RL Top (m AHD)	Start	End
2	Cell 2 Stage 2	408	412	1/10/2024	1/07/2025
1	Cell 1 Stage 3	411	414	1/7/2025	18/1/2026
2	Cell 2 Stage 3	412	414	18/1/2026	10/8/2026
1	Cell 1 Stage 4	414	418	10/8/2026	4/9/2027
2	Cell 2 Stage 4	414	418	4/9/2027	27/9/2028
3	Cell 3 Stage 1	399	418	27/9/2028	9/2/2030
1	Cell 1 Stage 5	418	420.5	9/2/2030	21/7/2030
2	Cell 2 Stage 5	418	420.5	21/7/2030	30/12/2030
3	Cell 3 Stage 2	418	420.5	30/12/2030	18/5/2031
1	Cell 1 Stage 6	420.5	423	18/5/2031	23/10/2031
2	Cell 2 Stage 6	420.5	423	23/10/2031	30/3/2032
5	MT Marven Pit	400.0	421	30/3/2032	12/5/2032
4	Cell 2B	406	432	12/5/2032	22/12/2034
3	Cell 3 Stage 3	420.5	423	22/12/2034	15/5/2035
5	MT Marven Pit	421.0	455	15/5/2035	20/9/2037

Table 4-2 Modelled seepage rates allocated in each TSF cell

Cell_ID	Total elemental area (m^2)	TSF Seepage rate (m3/day)	Model TSF seepage rate* (m/day)
1	68549.7	530	-0.00773
2	58607.0	530	-0.00904
3	74479.2	530	-0.00712
2B	90268.1	530	-0.00587
Mt Marvens	59694.6	530	-0.00888

* *Model inflows (2nd Type or Neumann boundary condition) in FEFLOW are conventionally negative (-ve).*

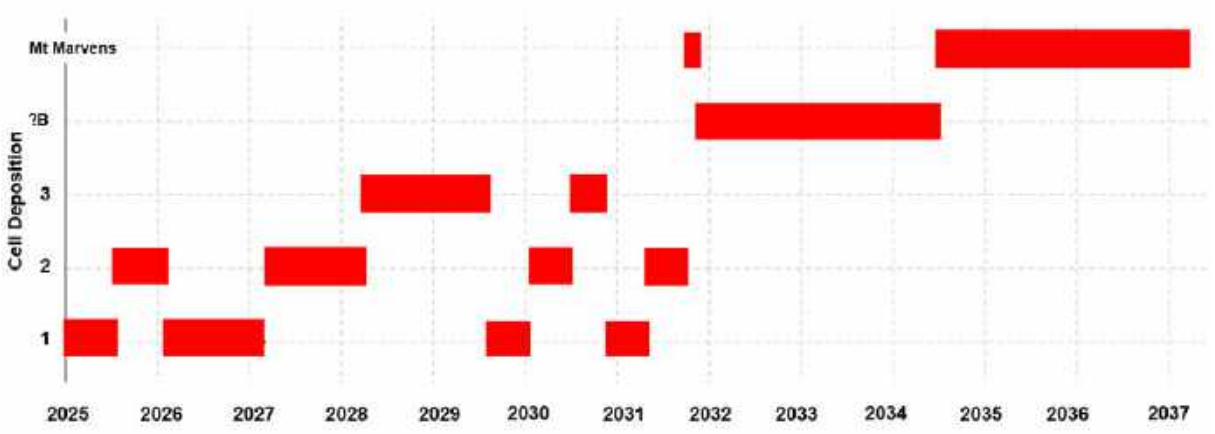

Figure 4-3 Visual graph of the deposition pattern in each TSF cell (Table 4-1)

A fixed-flow (Neumann-type) boundary condition was applied over each TSF pool footprint following the alternating deposition sequence shown in **Figure 3-2**. A nominal source concentration of 1,000 mg/L was assigned to the active TSF pool, while a background concentration of 10 mg/L was applied across the remainder of the model domain to represent uncontaminated groundwater. The solute was simulated as a conservative tracer, meaning it behaves as a highly mobile species transported solely by advection and hydrodynamic dispersion, with no attenuation through sorption, precipitation, or other geochemical reactions along the flow path.

In numerical groundwater models, reactive transport can be represented through sorption isotherms (e.g., linear, Langmuir) and associated retardation factors, which typically reduce solute migration rates relative to conservative tracers. However, reactive transport simulation is beyond the scope of this assessment and therefore the modelling adopts a conservative representation of contaminant behaviour.

Solute migration velocity is highly sensitive to the assumed effective (kinematic) porosity (ne) (De Marsily, 1986). Many modelling platforms, including FEFLOW, default to ne ≈ 0.30, implying that approximately one-third of pore volume contributes to advective transport—effectively equivalent to total porosity. Groundwater velocity is internally computed as the Darcy flux divided by ne; thus, lower porosity values produce higher advective transport velocities.

For this study, an effective porosity of 0.03 (3%) was adopted, consistent with site-specific estimates of specific yield (2–3%) for these formations. This parameterisation results in advective transport velocities approximately ten times faster than models using default porosity values, providing a conservative, worst-case assessment. Sensitivity analyses using alternative porosity values are presented in Section 4.3.

Dispersion parameters were assigned based on common groundwater modelling practice, recognising the scale-dependent nature of dispersivity. Longitudinal dispersivity was assigned approximately equal to the characteristic finite-element dimension, and transverse dispersivity was set to 10% of longitudinal dispersivity.

Consistent with a conservative approach, no extreme rainfall or enhanced recharge scenarios were applied. Instead, a spatially uniform recharge rate equal to the steady-state calibrated value was used for all simulations, representing conditions most favourable to plume mobility. To replicate groundwater stresses as realistically as possible, abstraction from the Calcrete and palaeochannel borefields remained active throughout the modelling period, consistent with Scenario 4 in Pennington Scott (2025).

4.2 Model results

4.2.1 Model Calibration - phase 1: 2018 to 2015

The objective of this simulation phase is to reproduce the most likely distribution of the solute plume from the TSFs over the period 2018 to 2025, which defines the before Genesis restart condition for the predictive scenario. This simulation includes operation of the Calcrete wellfield.

Initial groundwater levels were imported from the steady-state model, with a fixed water level of 315 m AHD applied at the Joanne Pit. A fixed inflow boundary was assigned to the TSF Cell 2 pool, introducing 530 m³/day of seepage water with a source concentration of 1,000 mg/L, while a background concentration of 10 mg/L was applied across the remaining model domain to represent uncontaminated conditions. A summary of the model configuration is presented in **Figure 4-2**. As described previously, an effective porosity of 0.03 (3%) was applied across the domain.

Water accumulating at the toe of the TSF embankments was removed via toe drains and sumps represented using seepage-face boundary conditions. Seepage-face elevations were set at 1.5 m below ground level for the toe drains and 2.0 m below ground level for the sumps. Recovery wells were included in the model design with fixed water levels 6 m below ground level, but were not activated in any scenario.

The seepage-face boundary condition is designed to simulate the hydraulic behaviour of engineered drains. When simulated groundwater levels exceed the assigned elevation, excess water is removed, constraining head to that elevation. When groundwater levels fall below the elevation, the boundary becomes inactive, allowing natural groundwater gradients to govern flow.

Results of this scenario, showing simulated groundwater levels and plume extent at the end of the calibration period, are presented in **Figure 4-4**. To aid visualisation of solute migration pathways, particle-tracking analysis was also undertaken (**Figure 4-5**). This analysis illustrates advective flow paths for hypothetical particles released at the TSF pool locations, representing transport governed solely by groundwater flow without dispersion or chemical reactions.

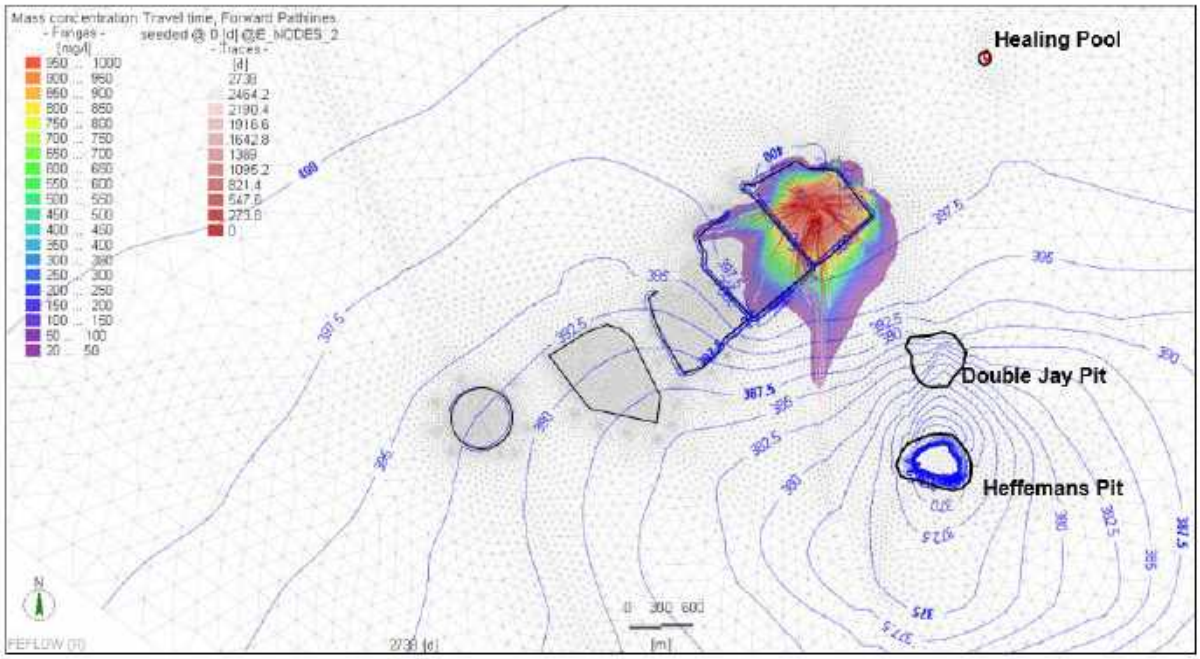

Figure 4-4 Calculated groundwater levels, concentrations and pathlines at the end of model phase 1 (June 2025)

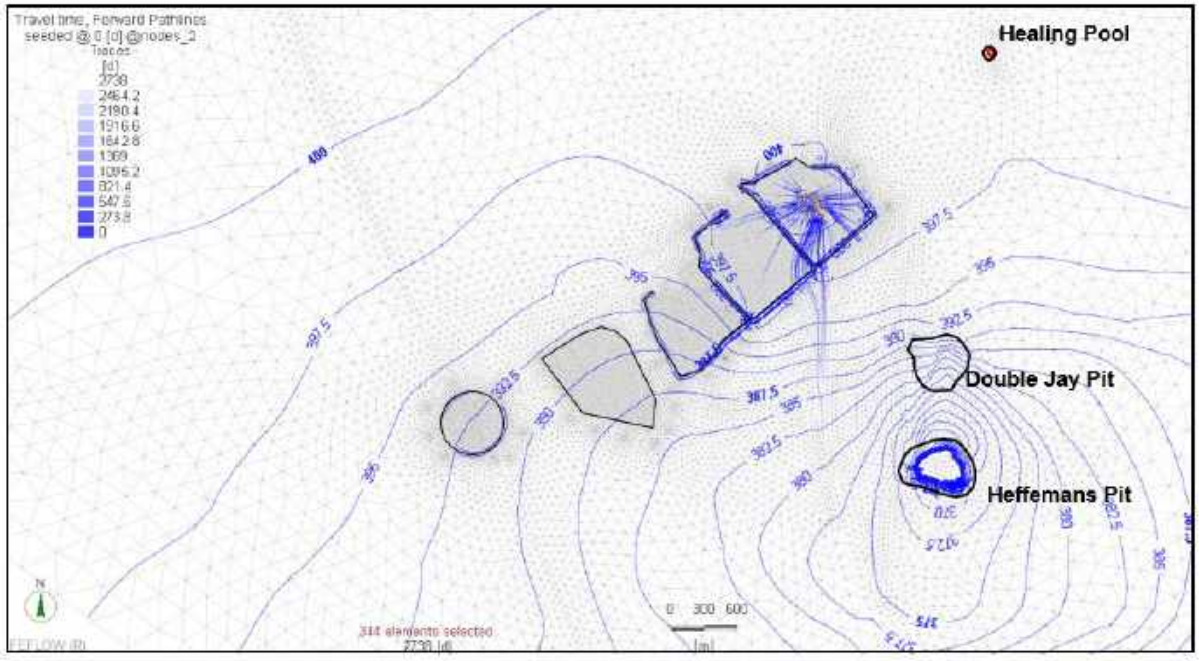

Figure 4-5 Flow path analysis over the period 2018 to 2025.

4.2.2 Model phase 2: Predictive scenario, 2025 to 2037.

The predictive scenario includes the model execution starting with initial groundwater and contaminant concentration the calculated values of the previous scenario. The results of this scenario are shown **Figure 4-6** through **Figure 4-8**.

Throughout the simulation, tailings are disposed in an alternating pattern and, based on the water balance analysis (CMW Geosciences, 2024), they infiltrate into the subsurface at an average seepage rate of 530 m^3/day (

Table 4-2).

The modelling results for this base-case scenario indicate that, under the specified assumptions, the contaminant plume, primarily originating from TSF Cells 1 and 2, migrates towards the void areas of the Heffernan's Pit. This movement follows the steep hydraulic gradients that have developed because of prolonged pit dewatering and are expected to persist at least until the completion of mining operations (end of 2037). The proposed sumps and toe drains located along the southern perimeter of the TSF cells are unable to fully intercept the solute plume due to the drawdown of groundwater levels towards the dewatering cone of depression.

There is low potential for solute migration eastward towards the Healing Pool, owing to the low hydraulic gradients in that direction, the operation of toe drains and sumps, and the relatively low hydraulic transmissivity of the playa and saprolite sediments underlying this area.

The solute plumes originating from TSF Cells 3, 2B, and Mt Marvan's Cell are expected to have limited spatial extent, reflecting the short operational duration of these cells.

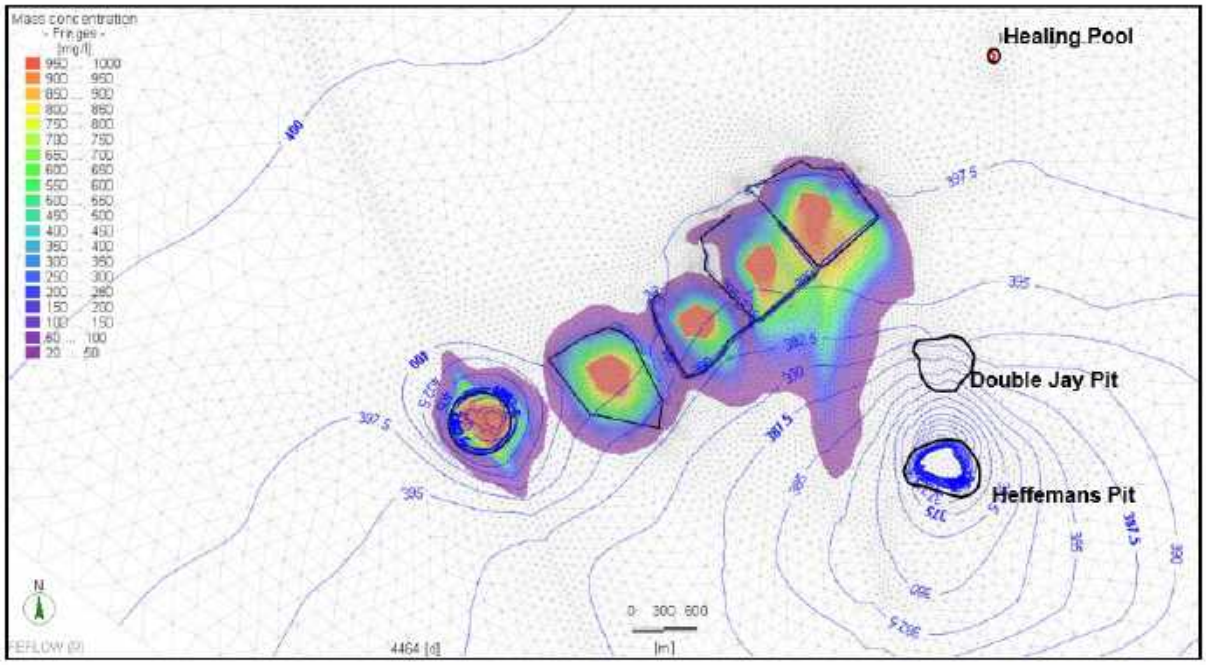

Figure 4-6 Groundwater levels, contaminant concentrations the end of model phase 2 (September 2037)

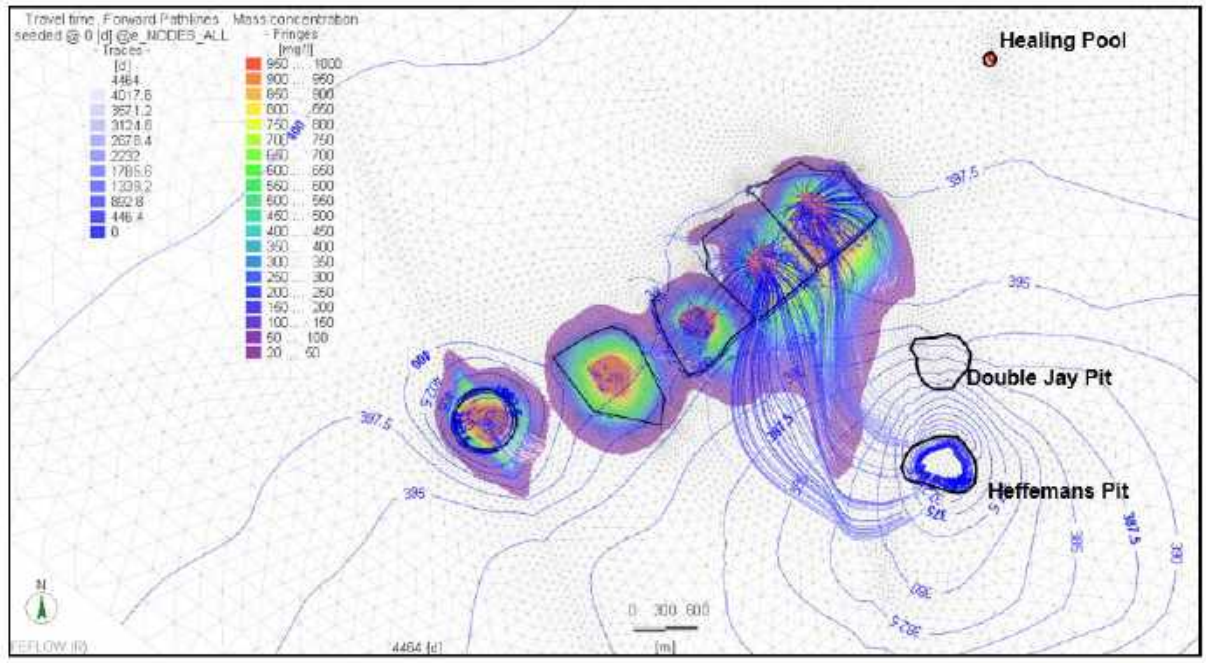

Figure 4-7 Groundwater levels, contaminant concentrations and pathlines (Sept. 2037)

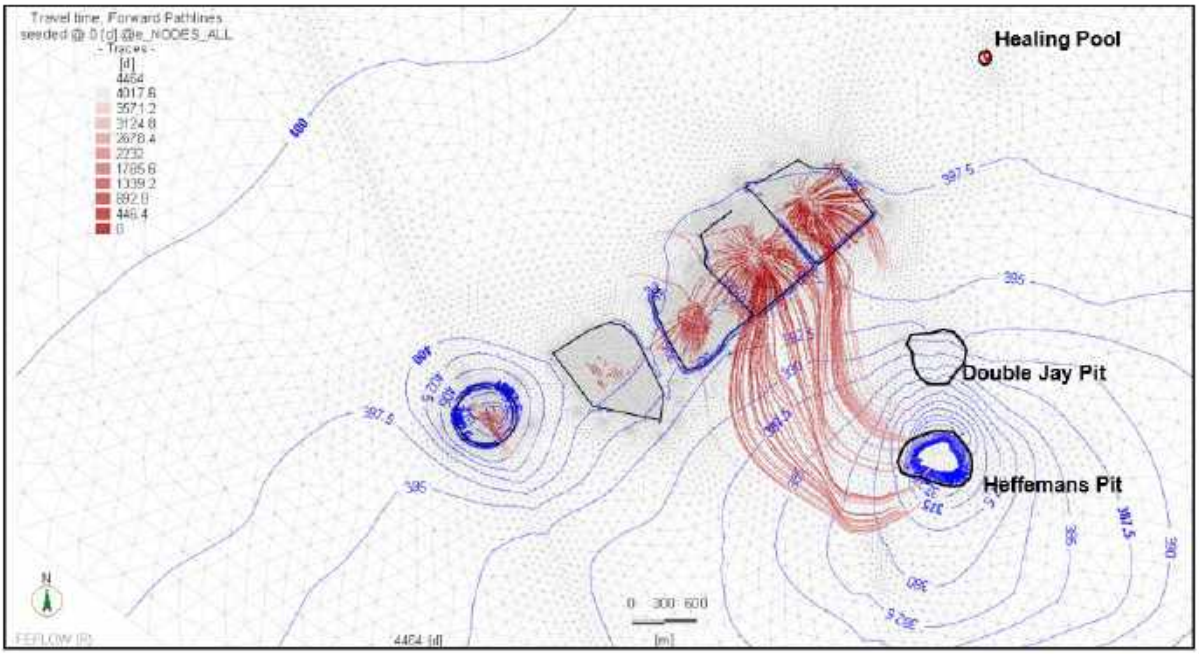

Figure 4-8 Flow path analysis over the period July 2025 to Sept. 2037.

4.3 Sensitivity & Uncertainty analysis

Predictive groundwater simulations are inherently subject to uncertainty, which generally falls into two primary categories:

1. **Structural Uncertainty** - arising from assumptions, data limitations, and simplifications used in developing the CSM in Pennington Scott (2025). This includes uncertainty in aquifer geometry, hydraulic properties, boundary conditions, and representation of flow processes.
2. **Uncertainty in Future Conditions** - associated with forecasting stresses and system responses, including future hydrological conditions, recharge rates, pumping schedules, and the timing and configuration of hydraulic sources and sinks. Broader non-hydrogeological influences such as economic drivers and regulatory or operational decisions also contribute to this uncertainty (Anderson, Woessner & Hunt, 2015).

Both categories are appropriately assessed through scenario-based modelling, which evaluates system response under alternative plausible future states and conceptual assumptions.

In contrast, calibration-constrained uncertainty analysis (e.g., using linear and non-linear techniques such as Monte Carlo methods or pilot-point parameterisation) is generally applied to highly parameterised models with extensive spatial datasets. Given the relatively low level of parameterisation in the current model and the spatially limited monitoring datasets, these approaches were not considered suitable or technically defensible for this application. Instead,

uncertainty has been addressed through targeted scenario simulations consistent with the model purpose and available data.

This report focuses primarily on solute-transport modelling, including the factors that control contaminant migration velocity and plume dispersion. Accordingly, the uncertainty analysis emphasises structural uncertainty and is implemented through scenario-based simulations. The key sources of uncertainty considered in this assessment are summarised below.

CMW Geosciences (2024) estimated an average seepage rate of 529.4 m³/day per TSF cell. While this estimate is supported by comprehensive geotechnical testing, laboratory characterisation, and numerical seepage modelling, uncertainties remain. These relate to:

- potential changes in tailings hydraulic properties associated with consolidation over time, and
- the likelihood of higher seepage rates under elevated operational pond levels.

To address these uncertainties, seepage rates were varied using multipliers of 1.5×, 2×, 3× and 4× the base rate (~530 m³/day). The influence of variable seepage on plume evolution is illustrated in **Figure 4-9** through **Figure 4-12**, with a combined summary presented in **Figure 4-13**.

Solute migration velocity in porous media is inversely proportional to effective (kinematic) porosity, ne (De Marsily, 1986). Numerical interfaces such as FEFLOW commonly default to ne ≈ 0.30, implying that 30% of pore volume contributes to advective transport, effectively the same as total porosity.

Groundwater migration velocity is calculated by dividing the simulated Darcy flux by ne; therefore, smaller values of ne yield faster advective transport.

A conservative ne value of 0.03 (3%) was adopted for this assessment, consistent with site-specific specific-yield values (2 to 3%). This selection yields groundwater velocities approximately an order of magnitude higher than would occur under default ne = 0.30 assumptions. Sensitivity simulations were also undertaken for ne = 0.01 and ne = 0.30. Model results demonstrating the effect of porosity variation are presented in **Figure 4-14 to Figure 4-17**, with a combined summary in **Figure 4-18**.

This version of the MMGO model adopts the same hydrostratigraphy, aquifer properties, and stress framework as the version in Pennington Scott (2025) but expands the model domain to incorporate the proposed Stage 3 borefield in the northeast. Mesh refinement was applied around the TSF to improve simulation accuracy for solute transport and ensure concurrent solution of the groundwater flow and solute-transport equations.

The model uses an Equivalent Porous Medium (EPM) representation. Fracture networks are not explicitly simulated; instead, fracture-dominated flow paths are represented as zones of relatively high hydraulic conductivity. As a result, stochastic variations in fracture geometry and connectivity, which may influence local inflow patterns, are not explicitly captured. Future refinements incorporating additional geological and hydrogeological data may further enhance predictive confidence.

Across all scenarios, including elevated seepage and low effective porosity, solute migration from the TSFs is directed toward the Heffernen's Pit, which functions as a local hydraulic sink due to ongoing dewatering.

Key outcomes include:

- Higher seepage rates increase solute plume size, predominantly to the south and west.
- Eastward solute migration remains limited due to low transmissivity, subdued hydraulic gradients, and effective interception by toe drains and sumps.
- Lower ne values (1–3%) produce faster solute migration toward the pit, while ne = 30% causes the solute to be contained largely beneath the TSF footprint.

The adopted ne = 3% represents a **conservative worst-case** parameterisation, conceptually accounting for advective transport through low-porosity fractured media.

In summary, the numerical modelling demonstrates that the solute migration from the TSF is captured within mine-affected groundwater flow regimes, with migration directed toward dewatered pit Jupiter Pit Complex voids. There is negligibly low risk of off-site contaminant transport from the Project.

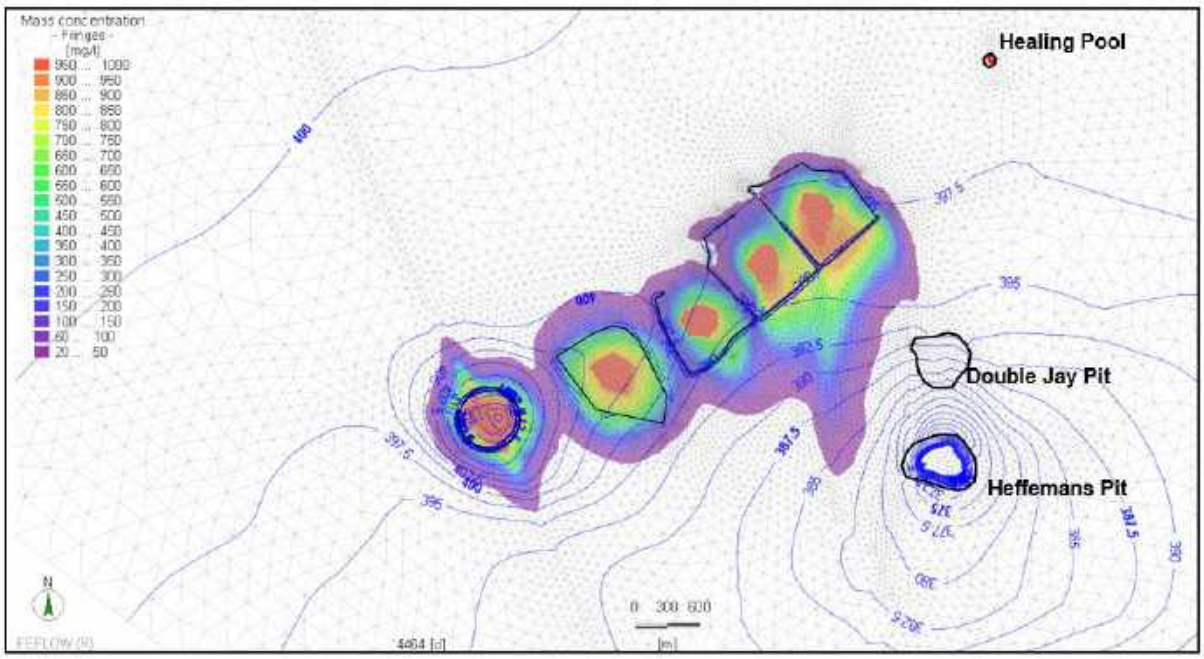

Figure 4-9 Distribution of the contaminant plume assuming seepage rate of 1.5 x base rate.

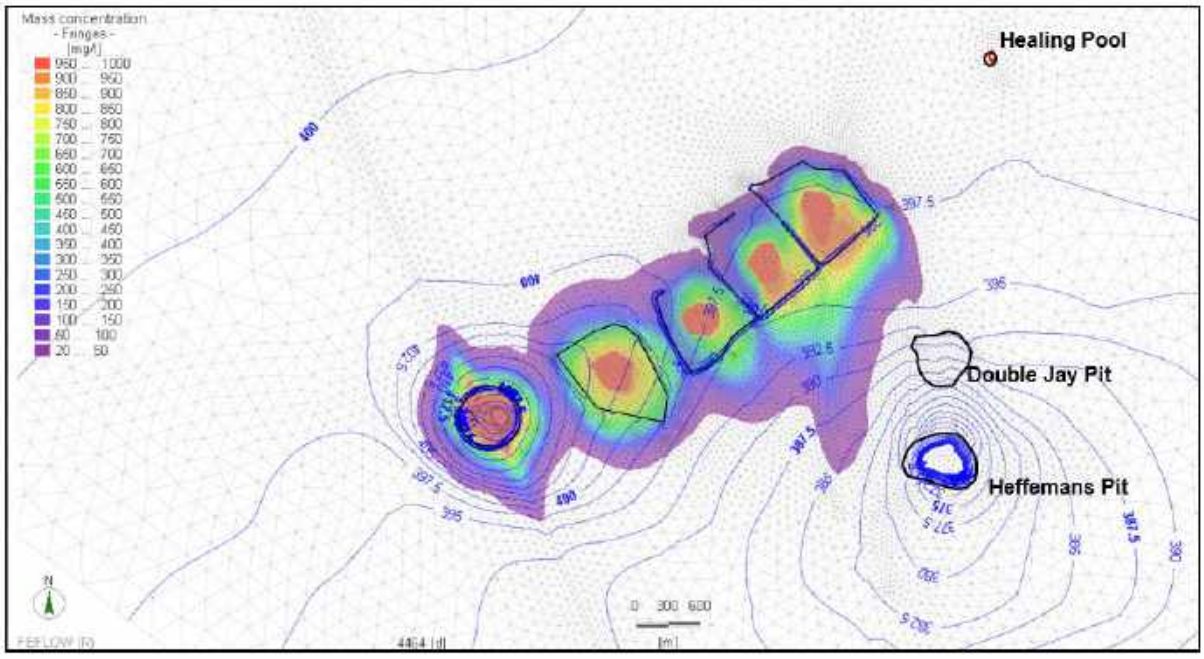

Figure 4-10 Distribution of the contaminant plume assuming seepage rate of 2.0 x base rate.

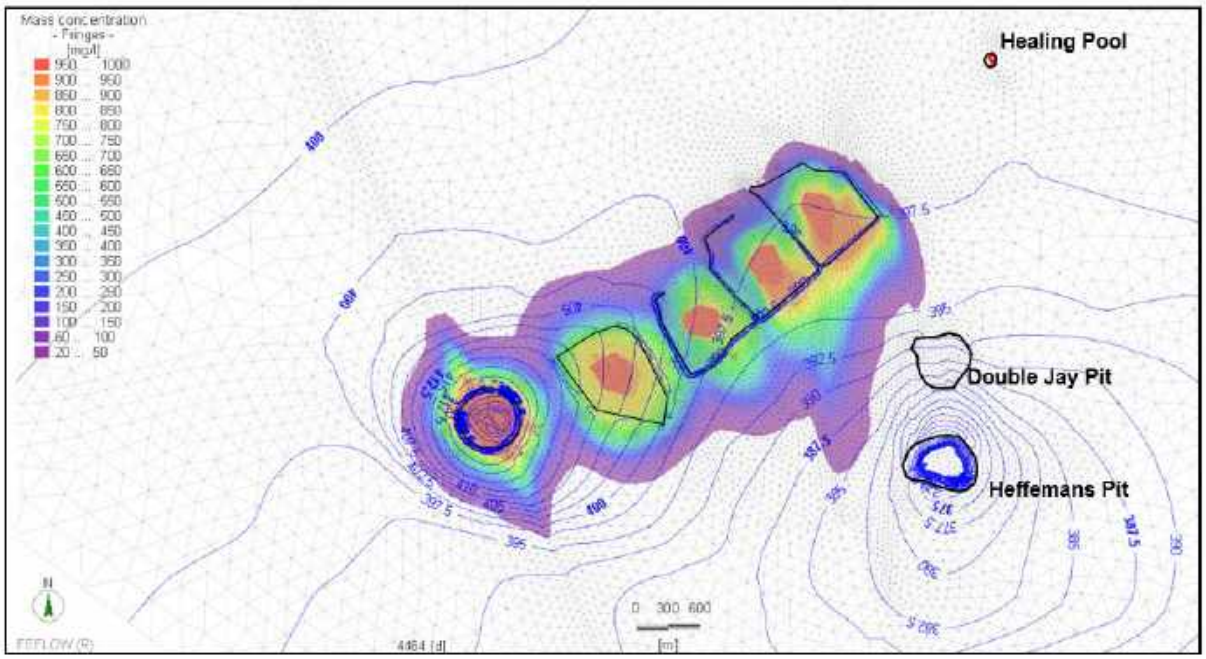

Figure 4-11 Distribution of the contaminant plume assuming seepage rate of 3.0 x base rate.

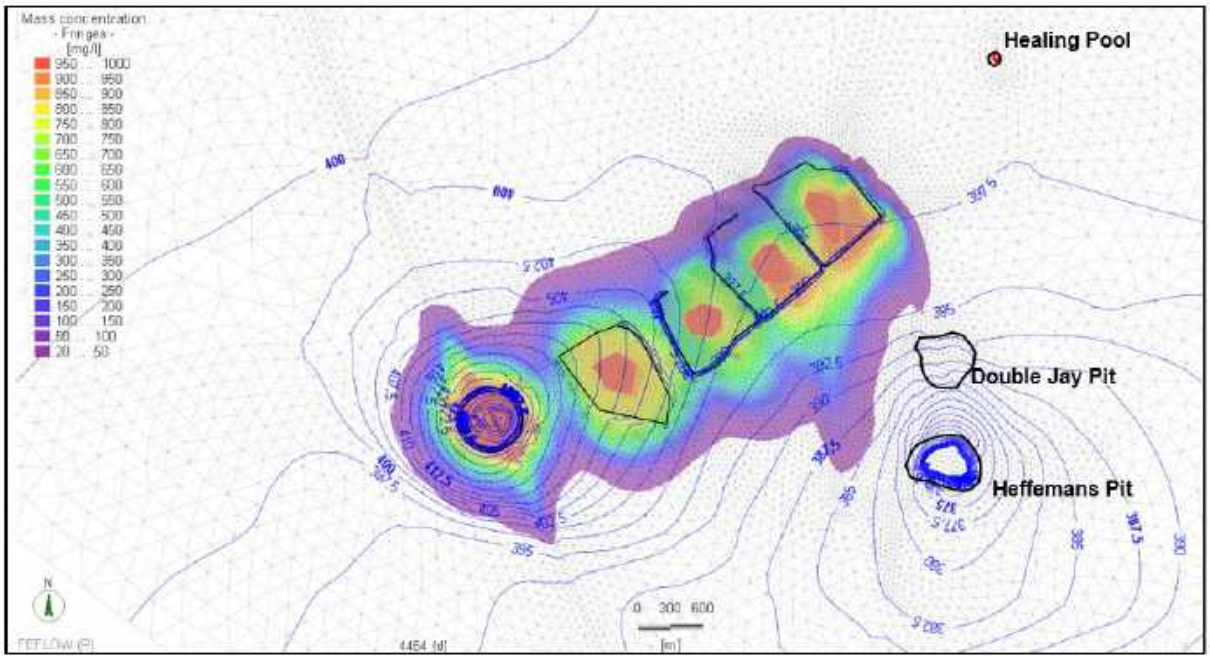

Figure 4-12 Distribution of the contaminant plume assuming seepage rate of 4.0 x base rate.

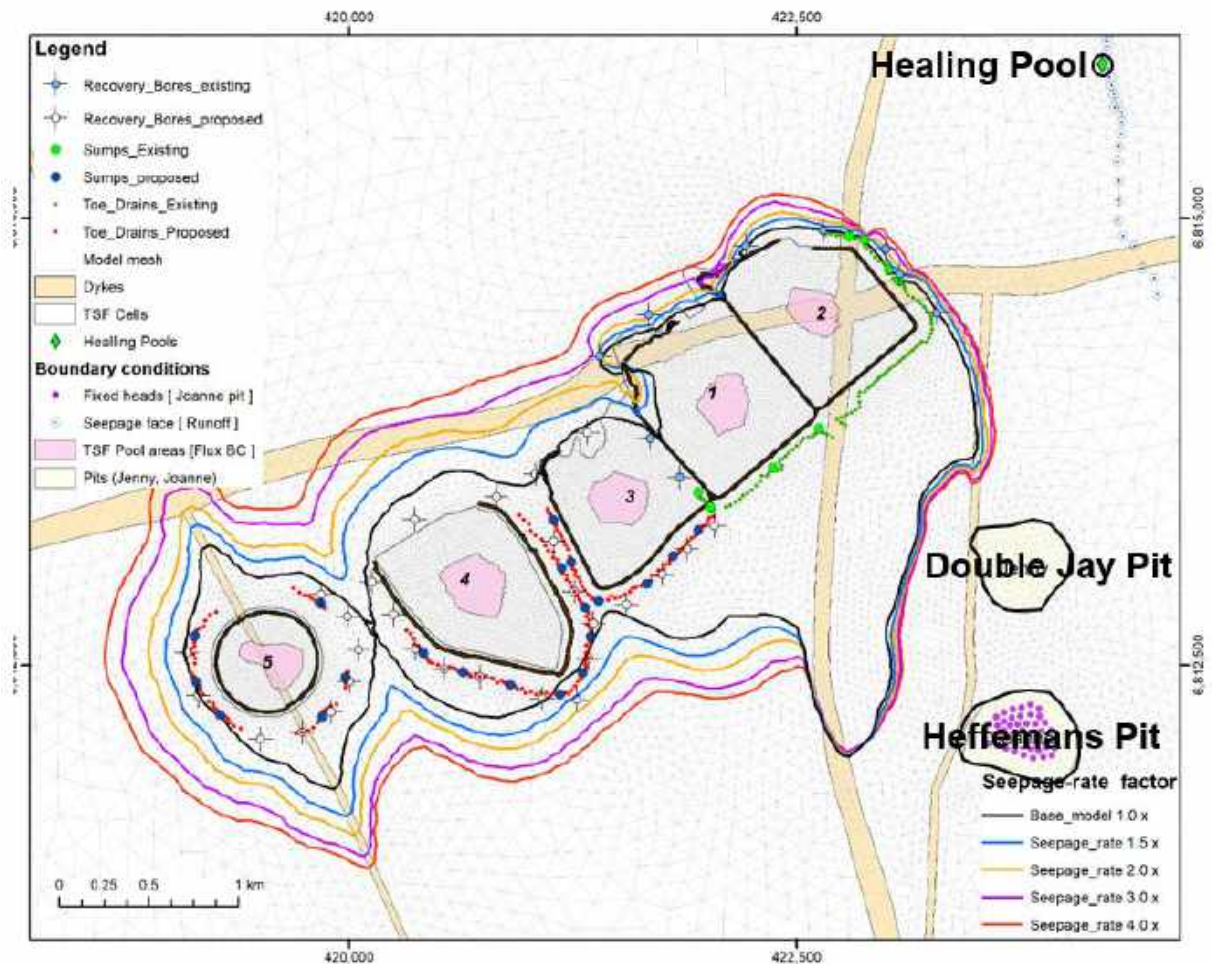

Figure 4-13 Comparison of plume extent (20 mg/L contour) at different multipliers of the base seepage rate of 530 m^3/day

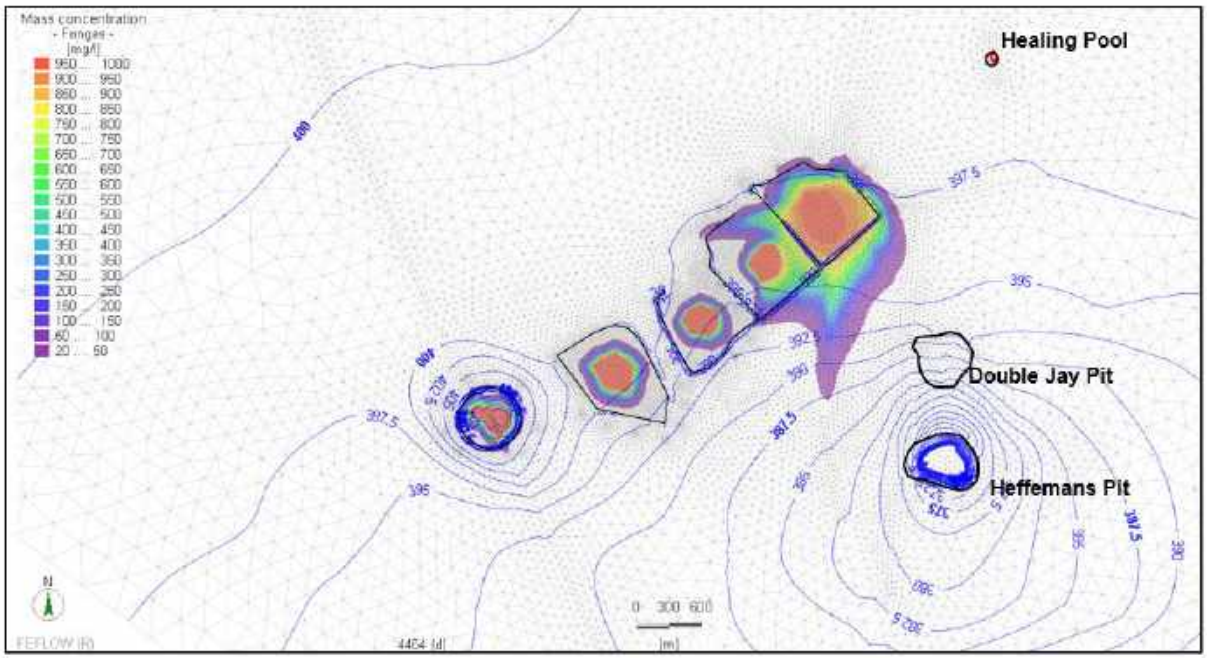

Figure 4-14 Distribution of the contaminant plume assuming effective porosity of 30 % (ne = 0.30)

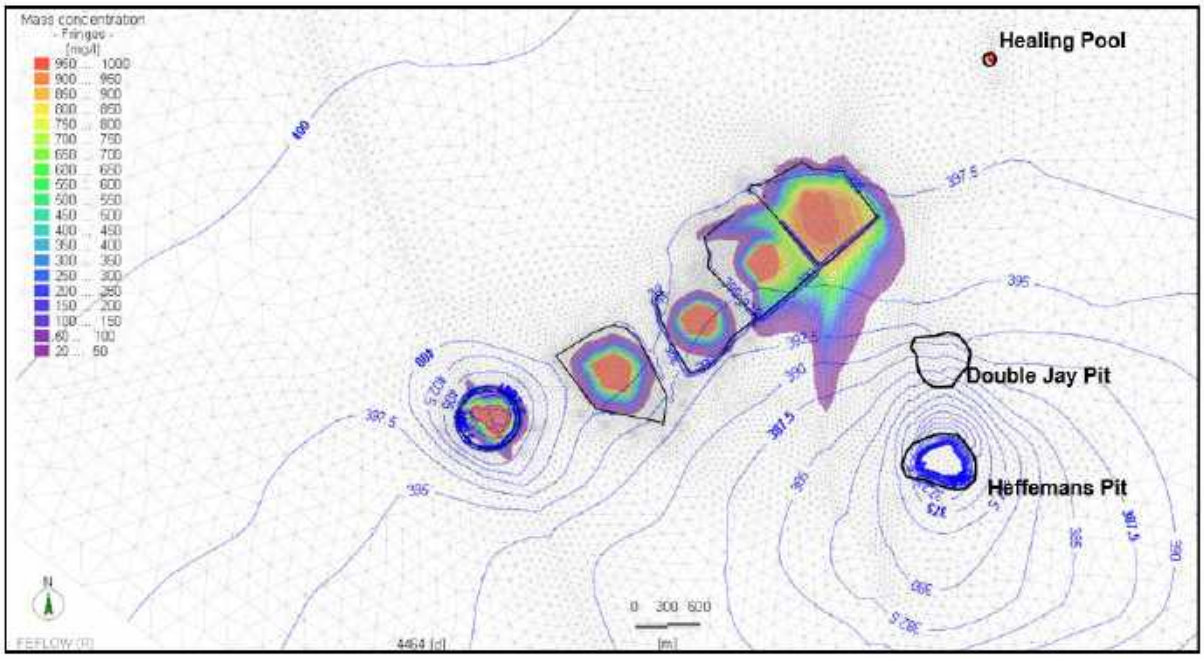

Figure 4-15 Distribution of the contaminant plume assuming effective porosity of 15 % (ne = 0.15)

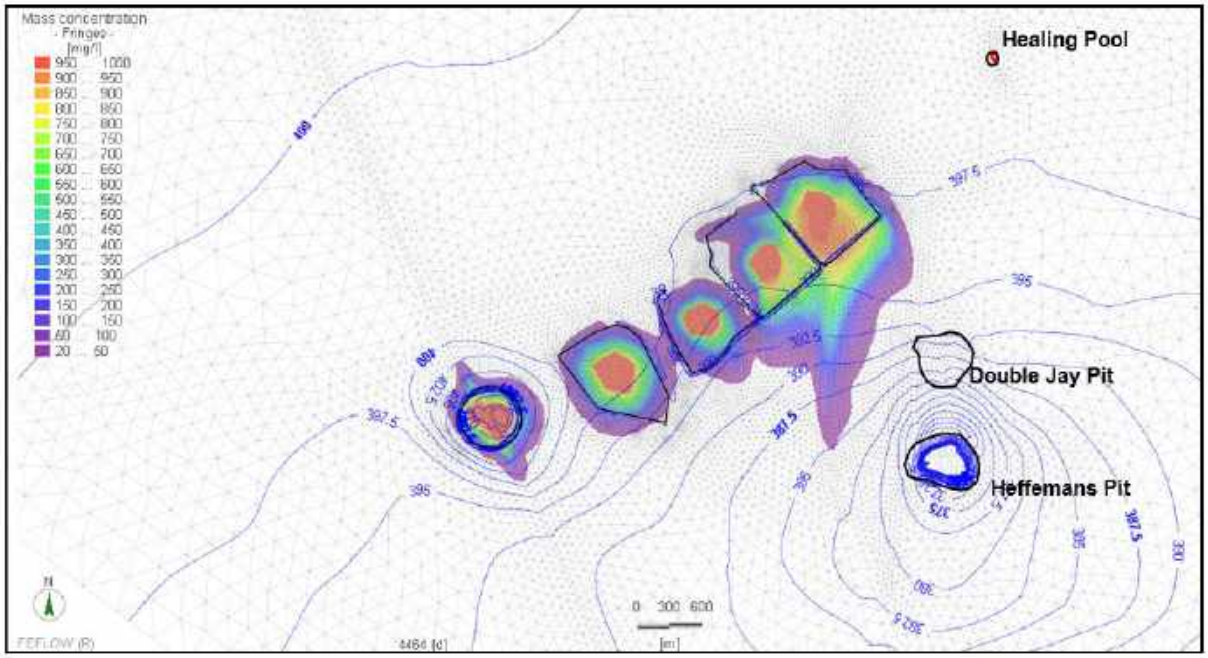

Figure 4-16 Distribution of the contaminant plume assuming effective porosity of 5% (ne = 0.05)

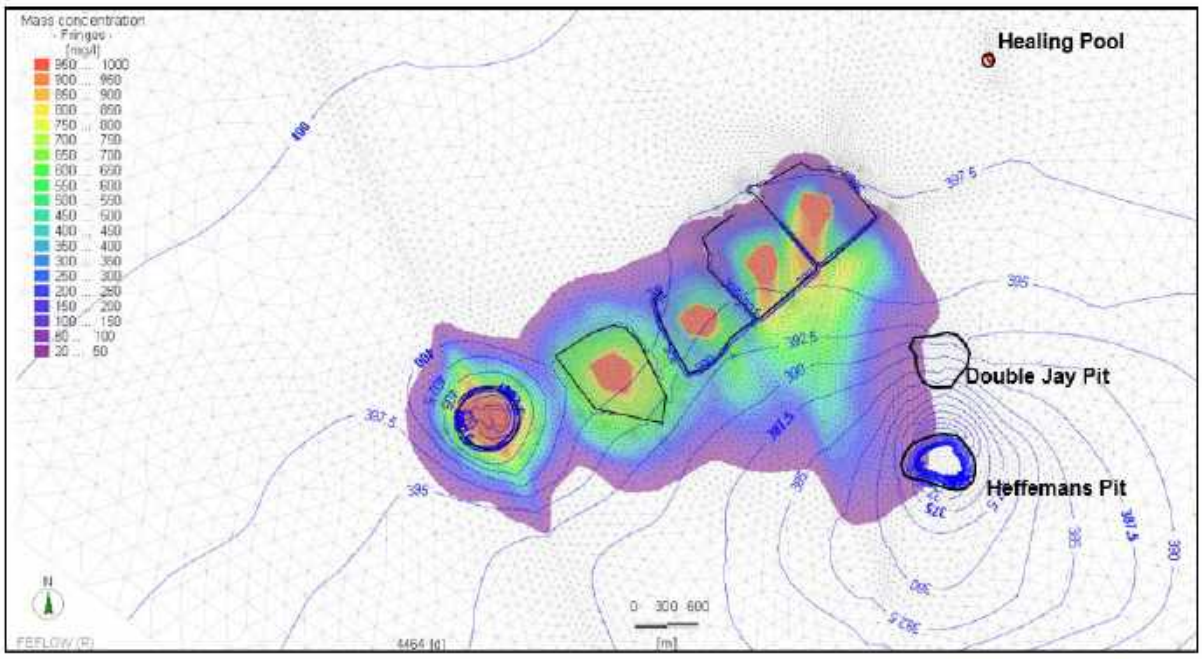

Figure 4-17 Distribution of the contaminant plume assuming effective porosity of 1 % (ne = 0.01)

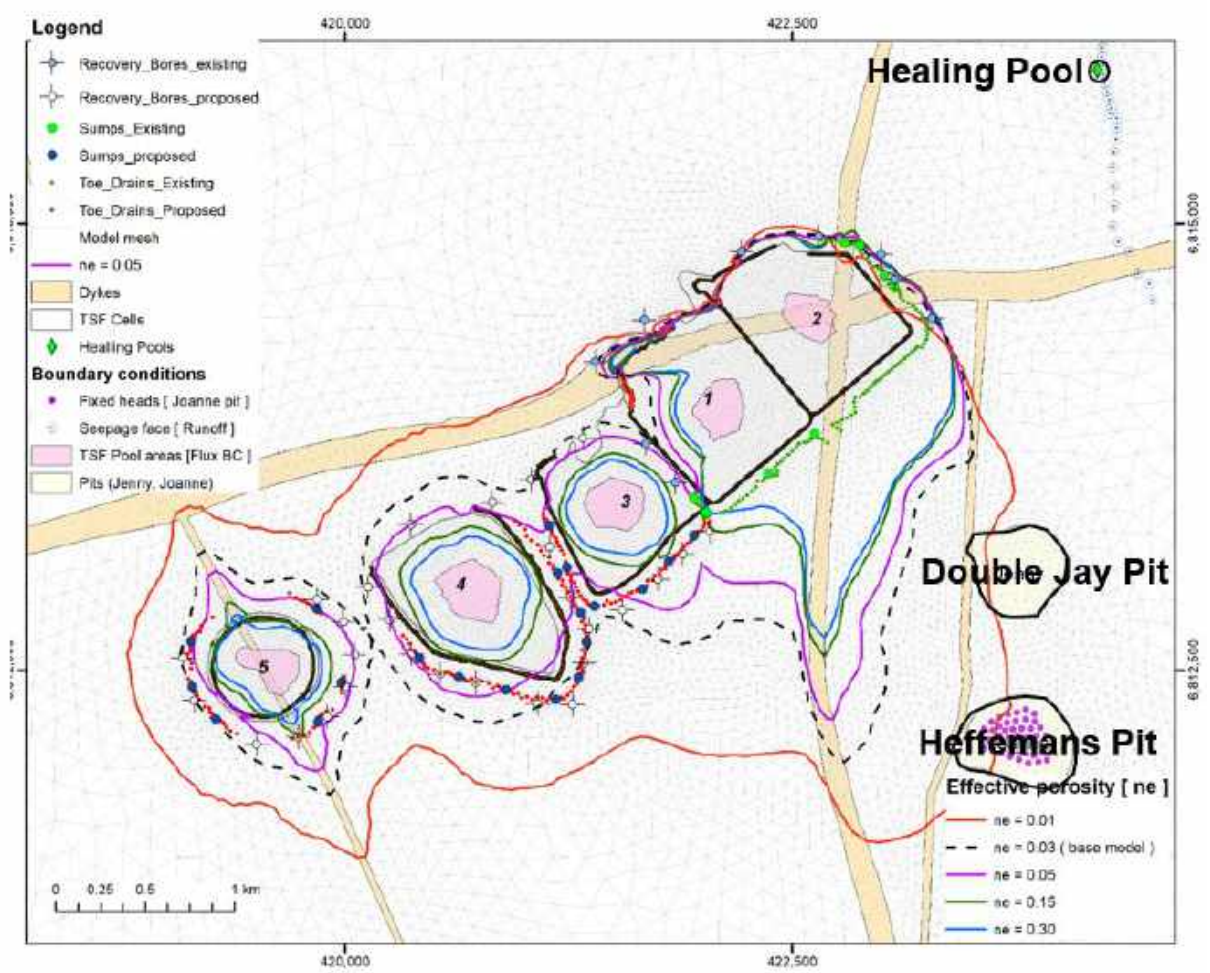

Figure 4-18 Comparison of plume extent (20 mg/L contour) at different values of effective (kinematic) porosity

5. CONCLUSIONS

During the previous operational phase of the Mt Morgans Gold Operation (**MMGO**) from March 2017 to March 2023, Dacian Gold deposited tailings from the 3 Mtpa Jupiter processing plant into Tailings Storage Facility (**TSF**) Cells 1 and 2. Genesis Minerals Limited (**Genesis**) recommissioned the Jupiter Plant in October 2024 and plans to increase throughput to 5 Mtpa by 2027. The TSF Project involves additional wall raises on Cells 1 and 2 and the construction of three new cells: Cell 3, Cell 2B, and the Mt Marven Cell. While Works Approvals have been issued for the Cell 1 and 2 raises, the new cells require further environmental and social impact assessment.

Seepage infiltration creates localised groundwater mounding beneath and immediately surrounding each TSF cell, with groundwater then migrating laterally toward zones of lower hydraulic head. Although TSF seepage (at 50,000 mg/L 120,000 mg/L) is less saline than that of the salt lake receiving environment (250,000 to 300,000 mg/L), it can contain additional solutes such as weak-acid dissociable (WAD) cyanide, nitrates, and trace metals. Metals tend to precipitate out of solution or adsorb to clays and organic matter within short distances of the TSF, whereas conservative (non-reactive) solutes, particularly chloride and nitrate, remain mobile and migrate the furthest along flow paths, with attenuation governed primarily by advection and dispersion processes.

To evaluate the fate and transport of the worst-case conservative solutes from the TSF, an existing regional groundwater flow model of MMGO dewatering and supply operations (Pennington Scott, 2025) was modified to simulate seepage and solute transport associated with the progressive development of all TSF cells. The model domain covers the MMGO restart period from October 2024 to October 2037 and assesses potential impacts on the surrounding hydrogeological system, including any risk to the Healing Pool.

The modelling was undertaken using the FEFLOW finite-element code to simulate coupled groundwater flow and solute transport, adopting an Equivalent Porous Medium (EPM) approach in which fracture networks are represented as zones of enhanced hydraulic conductivity within a porous matrix. Model geometry and hydraulic parameters were derived from the conceptual site model (CSM) described in Pennington Scott (2025), supported by borehole logs and the prior calibration dataset.

A base seepage rate of 530 m^3/day per cell was applied, consistent with CMW Geosciences (2024), with sensitivity simulations using multipliers of 1.5×, 2×, 3× and 4× to evaluate potential variability under different operational and hydraulic conditions. Solute transport was modelled conservatively (without retardation or chemical reactions) using a low effective porosity (n_e = 0.03), representing a worst-case scenario that maximises advective transport.

Sensitivity analyses show that higher seepage rates produce broader solute plumes extending predominantly southward and westward toward the dewatered pits, without altering the general direction of migration. Results are also sensitive to effective porosity: higher n_e values (~0.30) confine solute movement largely beneath the TSF footprint, whereas lower values (0.01–0.03) accelerate transport toward the pits. The adopted n_e = 0.03 aligns with measured specific-yield

values (2–3%) and provides a conservative representation of potential solute migration through the low-porosity fractured rock system.

Key findings from the solute transport modelling are summarised as follows:

- Migration direction: Solute transport from TSF Cells 1 and 2 occurs predominantly southward toward the Double Jay and Heffernan's Pits within the Jupiter Pit Complex, which functions as the principal hydraulic sink under continued dewatering.
- Hydraulic interception: Toe drains and collection sumps along the southern TSF embankments capture a portion of seepage; however, they do not fully offset the persistent drawdown gradients that drive groundwater flow toward the pits.
- Limited eastward migration: Solute movement toward the Healing Pool is negligible due to the very low transmissivity and subdued hydraulic gradients within the playa sediments and Lower Saprolite, combined with effective local drainage pathways.

In summary, even under highly conservative assumptions; including use of non-reactive solutes, elevated seepage rates, and low effective porosity, solute migration remains hydraulically constrained within the Jupiter Pit dewatering cone. The modelling indicates a very low likelihood of off-site migration under current or reasonably foreseeable operating conditions, and no credible pathway for solute movement toward the Healing Pool.

6. REFERENCES

ANDERSON, M. P., WOESSNER, W. W., & HUNT, R. 2015. Applied Groundwater Modelling. Simulation of Flow and Advective Transport. 533p. Elsevier.

BARNETT, B., TOWNLEY, L. R., POST, V., EVANS, R. E., HUNT, R. J., PEETERS, L., AND BORONKAY, A. 2012. Australian groundwater modelling guidelines. ISBN: 978-1-921853-91-3. Commonwealth of Australia 2012.

BOUWER H. 1978. Groundwater Hydrology. McGraw-Hill Book Company. 480p CMW GEGOSCIENCES 2023. Design Report for Tailings Storage Facility (TSF) Cells 1 and 2 + new Cell 3 on behalf of Dacian Gold Pty Ltd. PER2023-0063AC Rev 0

CMW GEOSCIENCES 2024. Tailings Storage Facility (TSF) Options Study. Mt Morgans Gold Project, Western Australia. Study report. Dacian Gold Ltd.

GLOVER R.E., 1964. The pattern of fresh-water flow in a coastal aquifer. In Sea water in coastal aquifers, USGS Water Supply Paper 1613-C, pp. C32-C35 GRM 6 Feb 2024a. Updated groundwater management plan for Mt Morgans Tailings Storage Facility. TM: J2402R01

GRM 6 Feb 2024b. Technical Memorandum regarding the second drilling program at the Mt Morgans tailings storage facility. TM: J2402TM02

HEIJDE, V. D. 1996. Systematic Evaluation and Testing of Groundwater Modelling Codes. International Groundwater Modelling Centre.

NATIONAL UNIFORM DRILLERS LICENSING COMMITTEE 2021. Minimum Construction Requirements for Water Bores in Australia Version 4.

PENNINGTON SCOTT Dec 2024. Bore Completion Report for Mount Morgans TSF Monitor bores on behalf of Genesis Minerals (Laverton) Limited. Report No 2410 Rev 0

PENNINGTON SCOTT. 2025. H3 Investigations for the MMGO Carey Palaeochannel Aquifer. Appendix E - Numerical Groundwater model.